IOPscience iopscience.iop.org

Home Search Collections Journals About Contact us My IOPscience

The Caldeira–Leggett quantum master equation in Wigner phase space: continued-fraction solution and application to Brownian motion in periodic potentials

This article has been downloaded from IOPscience. Please scroll down to see the full text article.

2004 J. Phys. A: Math. Gen. 37 10735

(http://iopscience.iop.org/0305-4470/37/45/003)

View the table of contents for this issue, or go to the journal homepage for more

Download details:
IP Address: 155.210.93.57
The article was downloaded on 25/06/2010 at 14:38

Please note that terms and conditions apply.

INSTITUTE OF PHYSICS PUBLISHING JOURNAL OF PHYSICS A: MATHEMATICAL AND GENERAL

J. Phys. A: Math. Gen. **37** (2004) 10735–10770 PII: S0305-4470(04)83801-0

The Caldeira–Leggett quantum master equation in Wigner phase space: continued-fraction solution and application to Brownian motion in periodic potentials

J L García-Palacios and D Zueco

Dep. de Física de la Materia Condensada e Instituto de Ciencia de Materiales de Aragón, C.S.I.C.—Universidad de Zaragoza, E-50009 Zaragoza, Spain

Received 19 July 2004
Published 28 October 2004
Online at stacks.iop.org/JPhysA/37/10735
doi:10.1088/0305-4470/37/45/003

Abstract

The continued-fraction method of solving classical Fokker–Planck equations has been adapted to tackle quantum master equations of the Caldeira–Leggett type. This was done taking advantage of the phase-space (Wigner) representation of the quantum density matrix. The approach differs from those in which some continued-fraction expression is found for a certain quantity, in that the full solution of the master equation is obtained by continued-fraction methods. This allows us to study in detail the effects of the environment (fluctuations and dissipation) on several classes of nonlinear quantum systems. We apply the method to the canonical problem of quantum Brownian motion in periodic potentials both for cosine and ratchet potentials (lacking inversion symmetry).

PACS numbers: 05.40.−a, 03.65.Yz, 05.60.−k

1. Introduction

The phase-space formulation of quantum mechanics has received renewed attention in the last few decades [1–3] because it allows one to employ notions and tools of classical physics in the quantum realm. The central object in this approach is *Wigner's function*

$$W(x,p)=\frac{1}{2\pi\hbar}\int \mathrm{d}y\,\mathrm{e}^{-\mathrm{i}py/\hbar}\varrho(x+\tfrac{1}{2}y,x-\tfrac{1}{2}y), \tag{1}$$

which is merely a phase-space (x, p) representation of the density matrix $\varrho(x,x')=\langle x|\hat{\varrho}|x'\rangle$. In a closed system, the dynamical equation for the Wigner function is equivalent to *Schrödinger's (or von Neumann) equation* while, in the $\hbar\to 0$ limit, it recovers *Liouville's equation* for the phase-space distribution in classical mechanics.

Another remarkable property of the Wignerian representation is the *average property*. The expectation value of a quantum operator $\hat{A}$ is obtained from the corresponding classical

 © 2004 IOP Publishing Ltd Printed in the UK

variable $A(x, p)$ (related to $\hat{A}$ by Weyl's rule; see [4], chapter 1) by a prescription analogous to the classical one, namely

$$\langle A\rangle \equiv \mathrm{Tr}(\hat{\varrho}\hat{A}) = \int \mathrm{d}x\,\mathrm{d}p\, W(x,p)A(x,p). \tag{2}$$

Thus, in spite of not being necessarily positive, the Wigner function can be considered as a sort of quantum mechanical 'distribution'. Besides, the marginal distributions of W give the true quantum probabilities of x, as $P(x) \equiv \langle x|\hat{\varrho}|x\rangle = \int \mathrm{d}p\, W(x,p)$, or of p, as $P(p) \equiv \langle p|\hat{\varrho}|p\rangle = \int \mathrm{d}x\, W(x,p)$. Therefore, the Wigner formalism provides a natural quantum–classical connection. This has been specially exploited in the search for quantum analogues of various classical effects (e.g., chaos) or in the problem of the fuzzy borders between the quantum and classical worlds [5].

In contact with the surrounding medium, the (open) system experiences dissipation, fluctuations and decoherence [6–8]. Typically, one is interested in a system consisting of a few relevant degrees of freedom coupled to its environment, or bath, which has a very large number of degrees of freedom (e.g., phonons, photons, nuclear spins, etc). The system is not necessarily microscopic, but it can be a mesoscopic system described by some collective variables which under appropriate conditions can behave quantum mechanically [9, 10]. Because of the genericity of these situations and the fundamental issues raised (e.g., approach to thermal equilibrium, dissipation in tunnelling and coherence, measurement problem), the study of *quantum dissipative systems* is of interest in several areas of physics and chemistry [11].

The dynamics of an open system can, in many cases, be formulated in terms of a *quantum master equation* for the (reduced) density matrix. In the Wigner representation this can be compactly written as $\partial_t W = \mathcal{L}W$, with $\mathcal{L}$ a certain evolution operator. Taking the classical limit, the master equation for a particle of mass M in a potential $V(x)$ goes over the Klein–Kramers equation [12, 13]

$$\partial_t W = [-(p/M)\partial_x + V'\partial_p + \gamma\partial_p(p + Mk_{\mathrm{B}}T\,\partial_p)]W \tag{3}$$

which is simply a *Fokker–Planck equation* in phase space. The first two terms (Poisson bracket) generate the classical reversible evolution (Liouville equation). The last term ('collision operator') accounts for irreversible effects due to the coupling to the environment (dissipation and fluctuations). The damping parameter γ measures the strength of the coupling to the bath, which is at temperature T. It is worth recalling that phase-space dynamics also includes problems reducible to 'mechanical' analogues: Josephson junctions, certain electrical circuits, chemical reactions, etc.

A suitable non-perturbative technique to solve classical Fokker–Planck equations of systems with few degrees of freedom is the *continued-fraction method* [14]. This is a special case of the expansion into complete sets (Grad's) method to solve kinetic equations in statistical mechanics [15]. In brief, the distribution is expanded into a series of orthogonal polynomials and, as a result, the kinetic equation is transformed into an *infinite set of coupled equations* for the expansion coefficients C_i. Approximate solutions are obtained by truncating the hierarchy of equations at various levels. To get manageable expressions, however, the truncation needs to be performed at a low level. In the continued-fraction method, instead of truncating directly, one seeks for a basis in which the range of index coupling is short (ideally, the equation for C_i involves C_{i-1}, C_i, and C_{i+1}). Then, the (differential) recurrence relations among the C_i can be solved by iterating a simple algorithm, the structure of which is like that of a continued fraction (appendix A). For the Klein–Kramers equation (3) the tridiagonal chain of coupled equations for the C_i is called the *Brinkman hierarchy* [16]. It has been solved by continued-fraction methods to study classical particles subjected to dissipation and fluctuations [14]. The method

has also been extended to rotational Brownian motion problems involving classical spins and dipoles (see [17] and references therein).

To deal with quantum dissipative systems, however, is a more delicate task [7]. To begin with, phenomenological quantization of dissipative systems poses fundamental problems (e.g., with the uncertainty and superposition principles). A rigorous route is to model the bath in a simple way, quantize it together with the system and eventually trace over the environmental variables. However, the resulting theoretical frameworks are technically involved. *Quantum master equations*, except for simple cases, are difficult to solve. An alternative is provided by *quantum state diffusion* methods (see [18]), where stochastic evolution equations for state vectors in Hilbert space are introduced as computational tools. Nevertheless, its implementation seems to be restricted to systems with discrete spectrum (e.g., oscillators, two-state systems, etc). Similarly, *quantum Langevin equations* [19] are of limited use beyond nearly harmonic systems. For an arbitrary system, there exist exact *path-integral* expressions for the evolution of the density matrix (involving the so-called *influence functional* that incorporates environmental effects) [6, 7]. However, those expressions are difficult to evaluate, even numerically, because the propagating function is highly oscillatory, rendering numerical methods unstable at long times. Finally, *quantum Monte Carlo* simulations can in principle always be used. Nevertheless, in spite of ongoing progress (see [18]), they are computationally complex and suffer from the (dynamical) sign problem.

This situation strongly motivates the development of *alternative methods* for quantum dissipative systems. Inspired on their suitability for classical systems, continued-fraction techniques have been developed for a number of problems. Shibata *et al* [20, 21] applied them to solve a c-number quantum Fokker–Planck equation for a spin in a dissipative environment. Vogel and Risken [22] employed continued-fraction methods to solve master equations in quantum nonlinear optics (see also [23]). Recently [24], this method has been extended to study genuine phase-space problems within the Wigner formalism. A generalization of the Brinkman hierarchy for quantum master equations of the Caldeira–Leggett type was presented. It was shown that the continued-fraction method for the classical problem can, in principle, be adapted to solve this hierarchy, yielding a promising technique to study several classes of nonlinear quantum systems subjected to environmental effects.

In this paper, we first present the details necessary for the derivation of the quantum hierarchies and discuss their solution by continued fractions. The approach is then implemented for the problem of quantum Brownian motion in periodic potentials (a demanding problem with (partly) continuous spectrum). Both the cosine and simple ratchet potentials (lacking inversion symmetry) are considered. For the former, a number of previous results are recovered (so testing the method) and extended, while the physical interpretations are revisited within the Wigner formalism. For particles in ratchet potentials we study the effects of finite damping (inertia) on the rectified velocities. The phenomenology is interpreted in terms of the interplay of thermal hopping, overbarrier wave reflection, and tunnelling. Results for non-equilibrium dynamics under oscillating forcing are also discussed, which show the combined effect of quantum phenomena, thermal activation and dissipation in a nonlinear system. A number of technical issues are consigned to the appendices.

2. Quantum master equations in phase space

We start from the following generic form for the quantum master equation in the Wigner representation [25–28]:

$$\partial_t W = \left[-\frac{p}{M}\partial_x + V'\partial_p + \partial_p(\gamma p + D_{pp}\partial_p) + D_{xp}\partial_{xp}^2 + \sum_{s=1}^{\infty} \frac{(\mathrm{i}\hbar/2)^{2s}}{(2s+1)!} V^{(2s+1)}\partial_p^{(2s+1)} \right] W. \tag{4}$$

The first three terms, identifying $D_{pp} = \gamma M k_B T$, give the classical Klein–Kramers equation (3). The mixed diffusion term $D_{xp}\partial^2_{xp}W$ is heuristically related to the colour of the quantum noise [29]. The series of derivatives $\partial_p^{(2s+1)}W$ (Wigner–Moyal term) gives the quantum contribution to the unitary evolution of the closed system. Conditions under which this series can be truncated are sometimes discussed to avoid dealing with an infinite-order partial differential equation. However, we shall fully keep this term because it can be especially important in nonlinear systems [30].

Conditions of validity for the master-equation description are discussed in [31–33]. Equations of the type of (4) can be derived modelling the particle surroundings as a *bath of oscillators* representing the normal modes of the environment. However, a number of assumptions are typically involved like semiclassical or high-temperature bath (rendering the kernels of the influence functional local in time), weak system-bath coupling (Born–Markov approximations), etc. Then, one would heuristically expect equation (4) being valid for small enough $\hbar\gamma/k_B T$. Notwithstanding this, the *structure* of the equation seems to be quite generic. Thus, a quantum master equation recently derived for strong coupling [34], and valid for all $\hbar\gamma/k_B T$, involves terms similar to those in (4) [with x-dependent coefficients and renormalized $V(x)$]. Besides, the phase-space representation of the celebrated Lindblad master equation is obtained by simply adding to (4) terms of the form $\partial_x(x\,W)$ and $\partial_x^2 W$ [35]. Most of these terms can be readily incorporated in the treatment below (indeed, the term $D_{xp}\partial^2_{xp}W$, absent in the original Caldeira–Leggett equation, is included to illustrate this). The same, in principle, would apply to possible extensions of the quantum master equation (4).

3. Preliminary manipulations of the master equation

Firstly, it is convenient to introduce appropriate scaled units. These are based on a characteristic length x_0 (e.g., the distance between the minima in a double-well oscillator, the period in a periodic potential) and a characteristic energy E_0 (e.g., a barrier height). Then one scales frequencies by $\omega_0 = (E_0/Mx_0^2)^{1/2}$, time by ω_0^{-1}, forces by $F_0 = E_0/x_0$, the action by $S_0 = E_0/\omega_0$, etc. On the other hand, D_{pp} ($=\gamma M k_B T$ in a high-T bath) is handled as an effective temperature $k_B T_{\rm eff} = D_{pp}/\gamma M$ and we introduce some convenient thermal rescalings via the associated frequency $\omega_T = (k_B T_{\rm eff}/Mx_0^2)^{1/2}$. Thus, in the equations p is scaled by $Mx_0\omega_T$, the potential and D_{xp} appear divided by $k_B T_{\rm eff}$, γ enters in the combination $\gamma_T = \gamma/\omega_T$, time is multiplied by ω_T, while the thermal de Broglie wavelength $\lambda_{\rm dB} = \hbar/(4Mk_B T_{\rm eff})^{1/2}$ enters divided by x_0.

Omitting any marks for the scaled quantities (but keeping in mind specially the thermal rescaling of t, $V(x)$ and p), the master equation is simply written as

$$\partial_t W = \left[-p\,\partial_x + V'\partial_p + \gamma_T\partial_p(p+\partial_p) + D_{xp}\partial^2_{xp} + \sum_{s=1}^{\infty}\kappa^{(s)}V^{(2s+1)}(x)\partial_p^{(2s+1)}\right]W \tag{5}$$

with the coefficient in the quantum sum given by

$$\kappa^{(s)} = (-1)^s\lambda_{\rm dB}^{2s}/(2s+1)!. \tag{6}$$

Planck's constant $\hbar$ is introduced in terms of the characteristic action $S_0 = E_0/\omega_0$ via the quantum parameter K (denoted $\bar{K}$ in [24]):

$$\hbar/S_0 = 2\pi/K, \qquad \lambda_{\rm dB} = \pi\gamma_T/\alpha, \qquad \alpha = (\gamma/\omega_0)K. \tag{7}$$

The second relation gives $\lambda_{\rm dB}$ in terms of the Kondo parameter α, related by the third one to our K. The classical limit is approached as $\hbar/S_0 \to 0$, i.e., letting $K \to \infty$.

Let us now introduce a splitting of the evolution operator $\mathcal{L}$ that will facilitate the calculation of the matrix elements required when expanding $W(x,p)$ into complete sets. On

inspecting equations (5) and (6), we see that extending the quantum sum down to $s = 0$, we obtain the part $V' \partial_p$ of the classical term. Thus, we can decompose $\mathcal{L}$ into the irreversible, kinetic and potential parts:

$$\partial_t W = (\mathcal{L}_{\rm ir} + \mathcal{L}_{\rm kin} + \mathcal{L}_{\rm v})W, \qquad \begin{cases} \mathcal{L}_{\rm ir} &= \gamma_T \partial_p (p + \partial_p), \\ \mathcal{L}_{\rm kin} &= -(p - D_{xp}\partial_p)\partial_x, \\ \mathcal{L}_{\rm v} &= \sum_{s \geqslant 0} \kappa^{(s)} V^{(2s+1)} \partial_p^{(2s+1)}. \end{cases} \tag{8}$$

This natural splitting has the advantage of dealing with $V(x)$ (the most problem-dependent part) in a unified way. Besides, we have grouped the term $\partial_p \partial_x$ with the kinetic term $p\,\partial_x$ because they are structurally similar.

4. Derivation of the quantum hierarchies

In the expansion into complete sets approach to solve kinetic equations, the distribution is expanded in an orthonormal basis $\{\psi_n\}$ and the coupled equations for the coefficients C_n derived ([15], p. 176). For the Klein–Kramers equation (3) one uses Hermite functions of p as basis ([36], section (4.4))

$$\psi_n(p) = r_n \mathrm{e}^{-p^2/4} H_n(p/\sqrt{2}), \qquad r_n = [(2\pi)^{1/2} 2^n n!]^{-1/2}. \tag{9}$$

One starts with the expansion in the momentum because, while the p dependence of the Hamiltonian is fully specified (kinetic energy $p^2/2M$), the potential part $V(x)$ depends on the problem. Thus, explicit manipulations can be done on the parts involving p, which are valid for any system. On the other hand, the Hermite basis has a number of advantages [14]; not the least is the handling of the derivatives ∂_p in the dynamical equation by means of the associated creation and annihilation operators $b = \partial_p + \frac{1}{2}p$ and $b^+ = -\partial_p + \frac{1}{2}p$ (this will prove very convenient in the quantum case).

For the Klein–Kramers equation the resulting equations for the expansion coefficients C_n are called the *Brinkman hierarchy* [14, 16]. This plays an important role in classical systems, both for analytical treatments—derivations of $1/\gamma$ expansions, etc—and to develop efficient non-perturbative numerical methods. In fact, it has the structure of a three-term recurrence relation which, after expansion in the position basis, can be solved by continued fractions. In what follows, we shall proceed in the quantum case following as closely as possible the steps of the classical limit.

4.1. Expansion in the momentum basis

We start by expanding the Wigner function as

$$W(x, p) = w \sum_n C_n(x)\psi_n(p), \qquad w = \frac{\mathrm{e}^{-\eta p^2/2}}{(2\pi)^{1/4}} \mathrm{e}^{-\Phi(x)}, \tag{10}$$

where we have extracted the Boltzmann-type factor w. This involves the auxiliary parameter $0 \leqslant \eta \leqslant 1/2$ and potential $\Phi(x)$, which is frequently chosen proportional to $V(x)$, i.e., $\Phi = \varepsilon V$. The results should not depend on the η or ε used, but these may (i) put parts of the evolution operator $\mathcal{L}$ in self-adjoint form and/or (ii) improve the stability and convergence of the eventual numerical implementation.

From the orthonormality of the $\psi_n(p)$, the expansion 'coefficients' can be written as $C_n = \int \mathrm{d}p\, \psi_n \sum_m C_m \psi_m = \int \mathrm{d}p\, \psi_n\, (W/w)$. Then, differentiating with respect to t and using

the evolution equation $\partial_t W = \mathcal{L}W$, we get the dynamical equations for C_n

$$\partial_t C_n = \sum_m \hat{\mathcal{Q}}_{nm} C_m, \qquad \hat{\mathcal{Q}}_{nm} = \int \mathrm{d}p\, \psi_n \overline{\mathcal{L}} \psi_m, \qquad \overline{\mathcal{L}} = w^{-1}\mathcal{L}w. \tag{11}$$

To get the matrix elements $\hat{\mathcal{Q}}_{nm}$, which are still operators on the x-dependence of C_m, one needs the $w^{-1}(\cdot)w$ transform of $\mathcal{L}$. This can be split as $\overline{\mathcal{L}} = \overline{\mathcal{L}}_{\rm ir} + \overline{\mathcal{L}}_{\rm kin} + \overline{\mathcal{L}}_{\rm v}$, with $\mathcal{L}_{\rm ir}$, $\mathcal{L}_{\rm kin}$, and $\mathcal{L}_{\rm v}$ given by equation (8). The transformation of these operators is done in appendix B, taking advantage of results for *normal ordering* of b and b^+ (which we use to express the ∂_p and p's in $\mathcal{L}$). Then, with the $\overline{\mathcal{L}}_{\rm ir}$, $\overline{\mathcal{L}}_{\rm kin}$, and $\overline{\mathcal{L}}_{\rm v}$ obtained, we compute their matrix elements between the ψ_n, getting the $\hat{\mathcal{Q}}_{nm}$. The details of this part of the calculation are given in appendix C.

Introducing the results obtained for $\hat{\mathcal{Q}}_{nm}$ into $\partial_t C_n = \sum_m \hat{\mathcal{Q}}_{nm} C_m$ one gets the following *quantum (Brinkman) hierarchy*:

$$\begin{aligned} -\partial_t C_n = & \sum_{s=0}^{[(n-1)/2]} [\Gamma_n^{s,-} V^{(2s+1)}] C_{n-(2s+1)} + \sqrt{(n-1)n}\,\gamma_- C_{n-2} \\ & + \sqrt{n} D^- C_{n-1} + \gamma_n C_n + \sqrt{n+1} D^+ C_{n+1} \\ & + \sqrt{(n+1)(n+2)}\,\gamma_+ C_{n+2} + \sum_{s=0}^{\infty} [\Gamma_{n+(2s+1)}^{s,+} V^{(2s+1)}] C_{n+(2s+1)}. \end{aligned} \tag{12}$$

The auxiliary (damping) parameters introduced read

$$\gamma_\pm = \gamma_T \eta_\pm (1-\eta_\pm), \qquad \gamma_n = \gamma_T [2n(\eta-\sigma) - \eta_+^2], \tag{13}$$

which involve the following η-related parameters (note the sign exchange):

$$\eta_\pm = \eta \mp \tfrac{1}{2}, \qquad \sigma = \eta_- \eta_+. \tag{14}$$

In equation (12), the operators on the x dependences are

$$D^\pm = d_\pm(\partial_x - \Phi'), \qquad d_\pm = 1 + \eta_\pm D_{xp}, \qquad \Delta = \sigma \lambda_{\rm dB}^2 \partial_x^2, \tag{15}$$

$$\Gamma_n^{s,\pm} = \eta_\pm^{2s+1} \kappa_n^{(s)}\, \mathrm{e}^{-\Delta/2}\, {}_1F_1(-m, 2s+2; \Delta), \qquad \kappa_n^{(s)} = \kappa^{(s)} \sqrt{n!/m!}. \tag{16}$$

Here $m = n - (2s+1)$, ${}_1F_1(a, c; z)$ is the confluent hypergeometric (Kummer) function ([37], chapter 13.6) and $\kappa^{(s)}$ is given by equation (6). It is important to note that the Γ_n^s act only on $V(x)$ not on the $C_m(x)$ (appendix B).

The quantum hierarchy (12) is equivalent to the Caldeira–Leggett master equation (4). Previously, several hierarchies had been derived [38–41], but the treatment was for closed (Hamiltonian) systems [38–40] or involved unsuitable bases like $\{p^n\}$ [38, 40, 41]. In contrast, our hierarchy of *Hermitian moments* constitutes a direct quantum generalization of the Brinkman hierarchy. To verify this, note that in the classical case only the $s = 0$ terms survive in the sums of (12) (appendix C). Then, setting the usual $\eta = 1/2$, equation (12) reduces to

$$\partial_t C_n = -[\sqrt{n}(D^- + V') C_{n-1} + n\gamma_T C_n + \sqrt{n+1} D^+ C_{n+1}], \tag{17}$$

which is indeed the celebrated hierarchy associated to the Klein–Kramers equation.

For potentials obeying $V^{(s)} \equiv 0$, $\forall s \geqslant S$, the quantum hierarchy (12) is a recurrence relation with coupling to a finite number of terms. Examples include the harmonic oscillator $V = \frac{1}{2} M\omega_0^2 x^2$ and the double-well (Duffing) oscillator $V = -\frac{1}{2} a x^2 + \frac{1}{4} b x^4$. Finite-coupling

recurrences are always reducible to three-term vector recurrences (appendix A) and solvable by continued fractions, as in the classical case. However, for non-polynomial $V(x)$, this approach is prevented by the infinite coupling range in the index n, consequence of the infinite series of p-derivatives $V^{(2s+1)}\,\partial_p^{(2s+1)}$ in the Wigner–Moyal term. In what follows, we shall exploit the expansion in the position basis to show how this problem can be circumvented.

4.2. Expansion in the position basis

Recall that the coefficients C_n are still functions of x. Inserting their expansion in an orthonormal basis $\{u_\alpha(x)\}$ into the quantum hierarchy (11), we get the generic form

$$C_n(x) = \sum_\alpha C_n^\alpha u_\alpha(x) \qquad \rightsquigarrow \qquad \frac{\mathrm{d}}{\mathrm{d}t}C_n^\alpha = \sum_m \sum_\beta (\hat{Q}_{nm})_{\alpha\beta} C_m^\beta, \tag{18}$$

with matrix elements $(B)_{\alpha\beta} = \int \mathrm{d}x\, u_\alpha^*\, \hat{B}(x, \partial_x)\, u_\beta$. To put (12) into the above form we just need to (i) substitute the operators (and x-dependent coefficients) by their matrix elements $(B)_{\alpha\beta}$, (ii) attach position superscripts to the C_n, and, finally, (iii) sum over them. On doing so, we get the *expanded quantum hierarchy*

$$\begin{aligned} -\frac{\mathrm{d}}{\mathrm{d}t}C_n^\alpha = {} & \sum_{s\geqslant 0}\sum_\beta [\Gamma_n^{s,-} V^{(2s+1)}]_{\alpha\beta} C^\beta_{n-(2s+1)} + \sqrt{(n-1)n}\sum_\beta \gamma_- \delta_{\alpha\beta} C^\beta_{n-2} \\ & + \sqrt{n}\sum_\beta D^-_{\alpha\beta} C^\beta_{n-1} + \sum_\beta \gamma_n \delta_{\alpha\beta} C^\beta_n + \sqrt{n+1}\sum_\beta D^+_{\alpha\beta} C^\beta_{n+1} \\ & + \sqrt{(n+1)(n+2)}\sum_\beta \gamma_+ \delta_{\alpha\beta} C^\beta_{n+2} + \sum_{s\geqslant 0}\sum_\beta [\Gamma^{s,+}_{n+(2s+1)} V^{(2s+1)}]_{\alpha\beta} C^\beta_{n+(2s+1)}. \end{aligned} \tag{19}$$

Considering that $D^\pm = d_\pm(\partial_x - \Phi')$ and $\Phi = \varepsilon V$, we see that to get all matrix elements involved we just need those of ∂_x and of $V^{(2s+1)}$, namely

$$(\partial_x)_{\alpha\beta} = \int \mathrm{d}x\, u_\alpha^* \partial_x u_\beta, \qquad V^{(2s+1)}_{\alpha\beta} = \int \mathrm{d}x\, u_\alpha^* V^{(2s+1)} u_\beta \tag{20}$$

because the Γ_n^s only increase the order of the potential derivatives.

The expanded hierarchy has the form of a system of ordinary differential equations, $\dot{C}_n^\alpha = \sum_{m\beta} Q^{\alpha\beta}_{nm}\, C_m^\beta$. If N and A are some large truncation indices for the bases $\{\psi_n(p)\}$ and $\{u_\alpha(x)\}$, we have a problem with $(N \times A)$ equations. One may be tempted to try direct Runge–Kutta integration or numerical diagonalization of the associated $(N \times A) \times (N \times A)$ matrix. However, the dimensions involved are typically very large, so that it is worth pursuing a continued-fraction treatment[1].

As mentioned before, the p-recurrence has a finite coupling range for polynomial potentials. For other potentials, with an appropriate choice of the basis $\{u_\alpha(x)\}$, the matrix elements in equation (20) may vanish when the second index β lies at a certain 'distance' of the first α. Then, the expanded hierarchy would be a recurrence relation in the position indices with a finite coupling range, also amenable for a continued-fraction treatment. To proceed in these cases, we just need to transform the two-index hierarchies into ordinary recurrence problems (i.e., with one index).

[1] Dynamical equations for the Wigner function have in any case been tackled by purely numerical methods, like (pseudo-) spectral methods for partial differential equations (see [42, 43] and references therein), or grid discretization usually followed by Runge–Kutta integration [44].

5. Matrix quantum hierarchies with one-index recurrences

In order to apply the continued-fraction method when finite coupling range in one of the indices is attained, we need to convert first the two-index recurrences into ordinary recursions. In the resulting one-index recurrences the coefficients will be matrices acting on appropriate vectors formed with the C_n^α.

5.1. Matrix quantum hierarchy: p-recurrence

The generic expanded form (18) can be converted into an *one-index* recurrence relation in the momentum index introducing the following vectors and matrices:

$$\frac{\mathrm{d}}{\mathrm{d}t}\boldsymbol{c}_n=\sum_m \mathbb{Q}_{nm}\boldsymbol{c}_m,\qquad \boldsymbol{c}_n=\begin{pmatrix} C_n^{-A}\\ \vdots\\ C_n^{A}\end{pmatrix},\qquad \mathbb{Q}_{nm}=\begin{pmatrix} (\hat{Q}_{nm})_{-A,-A}&\cdots&(\hat{Q}_{nm})_{-A,A}\\ \vdots&\ddots&\vdots\\ (\hat{Q}_{nm})_{A,-A}&\cdots&(\hat{Q}_{nm})_{A,A}\end{pmatrix}, \tag{21}$$

where $(\hat{Q}_{nm})_{\alpha\beta}=\int \mathrm{d}x\, u_\alpha^*\,\hat{Q}_{nm}\,u_\beta$. That is, for a fixed n one forms the column vector with all the C_n^α with $\alpha=-A,\ldots,A$ (this index may take positive and negative values). Similarly, for given (n,m), we build the matrix $Q_{nm}^{\alpha\beta}\equiv(\hat{Q}_{nm})_{\alpha\beta}$ with all indices α,β.

Before giving explicit expressions for the matrix coefficients we introduce the following notation: $\mathbb{Q}_n^{\pm s}=\mathbb{Q}_{n,n\pm s}$, $\mathbb{Q}_n^{\pm\pm}=\mathbb{Q}_{n,n\pm 2}$, $\mathbb{Q}_n^{\pm}=\mathbb{Q}_{n,n\pm 1}$, and $\mathbb{Q}_n=\mathbb{Q}_{n,n}$. Then, the matrix quantum hierarchy (21) can be written as

$$\begin{aligned}\frac{\mathrm{d}}{\mathrm{d}t}\boldsymbol{c}_n=&\sum_{s\geqslant 1}\mathbb{Q}_n^{-(2s+1)}\boldsymbol{c}_{n-(2s+1)}+\mathbb{Q}_n^{--}\boldsymbol{c}_{n-2}+\mathbb{Q}_n^{-}\boldsymbol{c}_{n-1}+\mathbb{Q}_n\boldsymbol{c}_n+\mathbb{Q}_n^{+}\boldsymbol{c}_{n+1}\\&+\mathbb{Q}_n^{++}\boldsymbol{c}_{n+2}+\sum_{s\geqslant 1}\mathbb{Q}_n^{+(2s+1)}\boldsymbol{c}_{n+(2s+1)}.\end{aligned} \tag{22}$$

We have accounted for $\mathbb{Q}_n^{\pm(2s)}\equiv 0$, $\forall s\geqslant 2$ (see equation (19)) and incorporated the $s=0$ terms into the central $\boldsymbol{c}_{n\pm1}$ ones. The matrix coefficients explicitly read

$$\begin{cases}(\mathbb{Q}_n^{-(2s+1)})_{\alpha\beta}=-[\Gamma_n^{s,-}V^{(2s+1)}]_{\alpha\beta},\\ (\mathbb{Q}_n^{--})_{\alpha\beta}=-\sqrt{(n-1)n}\,\gamma_-\delta_{\alpha\beta},\\ (\mathbb{Q}_n^{-})_{\alpha\beta}=-\sqrt{n}\,D^-_{\alpha\beta}-[\Gamma_n^{0,-}V']_{\alpha\beta},\\ (\mathbb{Q}_n)_{\alpha\beta}=-\gamma_n\delta_{\alpha\beta},\\ (\mathbb{Q}_n^{+})_{\alpha\beta}=-\sqrt{n+1}\,D^+_{\alpha\beta}-[\Gamma_{n+1}^{0,+}V']_{\alpha\beta},\\ (\mathbb{Q}_n^{++})_{\alpha\beta}=-\sqrt{(n+1)(n+2)}\,\gamma_+\delta_{\alpha\beta},\\ (\mathbb{Q}_n^{+(2s+1)})_{\alpha\beta}=-[\Gamma_{n+(2s+1)}^{s,+}V^{(2s+1)}]_{\alpha\beta}.\end{cases} \tag{23}$$

For finite coupling range in n (e.g., in polynomial potentials), the hierarchy (22) is a recurrence relation to which continued-fraction methods can now be applied. This amounts to converting the underlying large $(N\times A)\times(N\times A)$ problem into N problems with associated $A\times A$ matrices [or $A\to(2A+1)$]. As the recursion 'coefficients' are matrices, one would need *matrix continued-fraction* methods (appendix A).

5.2. Matrix quantum hierarchy: x-recurrence

When the p-recurrence has an infinite coupling range (in periodic potentials, the Morse potential, etc), we can convert the two-index hierarchy (18) into matrix form, but introducing recurrences in the position index α

$$\frac{\mathrm{d}}{\mathrm{d}t}\boldsymbol{c}_\alpha = \sum_\beta \mathbb{Q}_{\alpha\beta}\boldsymbol{c}_\beta, \qquad \boldsymbol{c}_\alpha = \begin{pmatrix} C_0^\alpha \\ \vdots \\ C_N^\alpha \end{pmatrix}, \qquad \mathbb{Q}_{\alpha\beta} = \begin{pmatrix} (\hat{Q}_{00})_{\alpha\beta} & \cdots & (\hat{Q}_{0N})_{\alpha\beta} \\ \vdots & \ddots & \vdots \\ (\hat{Q}_{N0})_{\alpha\beta} & \cdots & (\hat{Q}_{NN})_{\alpha\beta} \end{pmatrix}. \tag{24}$$

That is, $(\mathbb{Q}_{\alpha\beta})_{nm} = (\hat{Q}_{nm})_{\alpha\beta}$, with $B_{\alpha\beta} = \int \mathrm{d}x\, u_\alpha^* \hat{B}\, u_\beta$. Thus, for a fixed α one constructs the column vector with the C_n^α for all $n = 0, \ldots, N$, and for given (α, β), the matrix $Q_{nm}^{\alpha\beta} \equiv (\hat{Q}_{nm})_{\alpha\beta}$ with all n, m. Comparing the matrix in (24) with equation (23) for $(\mathbb{Q}_n^{\pm s})_{\alpha\beta}$, we can construct $\mathbb{Q}_{\alpha\beta}$ diagonal by diagonal

$$\begin{cases} (\mathbb{Q}_{\alpha\beta})_{n,n-(2s+1)} = -[\Gamma_n^{s,-} V^{(2s+1)}]_{\alpha\beta}, \\ (\mathbb{Q}_{\alpha\beta})_{n,n-2} = -\sqrt{(n-1)n}\,\gamma_-\delta_{\alpha\beta}, \\ (\mathbb{Q}_{\alpha\beta})_{n,n-1} = -\sqrt{n}D_{\alpha\beta}^- - [\Gamma_n^{0,-} V']_{\alpha\beta}, \\ (\mathbb{Q}_{\alpha\beta})_{n,n} = -\gamma_n\delta_{\alpha\beta}, \\ (\mathbb{Q}_{\alpha\beta})_{n,n+1} = -\sqrt{n+1}D_{\alpha\beta}^+ - [\Gamma_{n+1}^{0,+} V']_{\alpha\beta}, \\ (\mathbb{Q}_{\alpha\beta})_{n,n+2} = -\sqrt{(n+1)(n+2)}\,\gamma_+\delta_{\alpha\beta}, \\ (\mathbb{Q}_{\alpha\beta})_{n,n+(2s+1)} = -[\Gamma_{n+(2s+1)}^{s,+} V^{(2s+1)}]_{\alpha\beta} \end{cases} \tag{25}$$

all other diagonals being zero $(\mathbb{Q}_{\alpha\beta})_{n,n\mp 2s} \equiv 0$, $\forall s \geqslant 2$.

To recognize better the structure of these matrices, we decompose them into the 'free' and potential contributions $\mathbb{Q}_{\alpha\beta} = \mathbb{Q}_{\alpha\beta}^{\mathrm{f}} + \mathbb{Q}_{\alpha\beta}^{\mathrm{v}}$. For $\mathbb{Q}_{\alpha\beta}^{\mathrm{f}}$, including the kinetic and irreversible terms, we have the pentadiagonal structure (tridiagonal for $\eta = 1/2$)

$$\mathbb{Q}_{\alpha\beta}^{\mathrm{f}} = -\begin{pmatrix} \gamma_0\delta_{\alpha\beta} & \sqrt{1}D_{\alpha\beta}^+ & \sqrt{1\cdot 2}\,\gamma_+\delta_{\alpha\beta} & 0 & 0 & 0 & \ddots \\ \sqrt{1}D_{\alpha\beta}^- & \gamma_1\delta_{\alpha\beta} & \sqrt{2}D_{\alpha\beta}^+ & \sqrt{2\cdot 3}\,\gamma_+\delta_{\alpha\beta} & 0 & 0 & \ddots \\ \sqrt{1\cdot 2}\,\gamma_-\delta_{\alpha\beta} & \sqrt{2}D_{\alpha\beta}^- & \gamma_2\delta_{\alpha\beta} & \sqrt{3}D_{\alpha\beta}^+ & \sqrt{3\cdot 4}\,\gamma_+\delta_{\alpha\beta} & 0 & \ddots \\ 0 & \sqrt{2\cdot 3}\,\gamma_-\delta_{\alpha\beta} & \sqrt{3}D_{\alpha\beta}^- & \gamma_3\delta_{\alpha\beta} & \sqrt{4}D_{\alpha\beta}^+ & \sqrt{4\cdot 5}\,\gamma_+\delta_{\alpha\beta} & \ddots \\ 0 & 0 & \sqrt{3\cdot 4}\,\gamma_-\delta_{\alpha\beta} & \sqrt{4}D_{\alpha\beta}^- & \gamma_4\delta_{\alpha\beta} & \sqrt{5}D_{\alpha\beta}^+ & \ddots \\ 0 & 0 & 0 & \sqrt{4\cdot 5}\,\gamma_-\delta_{\alpha\beta} & \sqrt{5}D_{\alpha\beta}^- & \gamma_5\delta_{\alpha\beta} & \ddots \\ \ddots & \ddots & \ddots & \ddots & \ddots & \ddots & \ddots \end{pmatrix}.$$

The part due to $V(x)$, on the other hand, has the following alternate dense structure, reflecting the odd powers of ∂_p in the Wigner–Moyal term:

$$\mathbb{Q}^{\mathrm{v}}_{\alpha\beta} = -\begin{pmatrix} 0 & [\Gamma_1^{0,+}V']_{\alpha\beta} & 0 & [\Gamma_3^{1,+}V^{(3)}]_{\alpha\beta} & 0 & [\Gamma_5^{2,+}V^{(5)}]_{\alpha\beta} & \ddots \\ [\Gamma_1^{0,-}V']_{\alpha\beta} & 0 & [\Gamma_2^{0,+}V']_{\alpha\beta} & 0 & [\Gamma_4^{1,+}V^{(3)}]_{\alpha\beta} & 0 & \ddots \\ 0 & [\Gamma_2^{0,-}V']_{\alpha\beta} & 0 & [\Gamma_3^{0,+}V']_{\alpha\beta} & 0 & [\Gamma_5^{1,+}V^{(3)}]_{\alpha\beta} & \ddots \\ [\Gamma_3^{1,-}V^{(3)}]_{\alpha\beta} & 0 & [\Gamma_3^{0,-}V']_{\alpha\beta} & 0 & [\Gamma_4^{0,+}V']_{\alpha\beta} & 0 & \ddots \\ 0 & [\Gamma_4^{1,-}V^{(3)}]_{\alpha\beta} & 0 & [\Gamma_4^{0,-}V']_{\alpha\beta} & 0 & [\Gamma_5^{0,+}V']_{\alpha\beta} & \ddots \\ [\Gamma_5^{2,-}V^{(5)}]_{\alpha\beta} & 0 & [\Gamma_5^{1,-}V^{(3)}]_{\alpha\beta} & 0 & [\Gamma_5^{0,-}V']_{\alpha\beta} & 0 & \ddots \\ \ddots & \ddots & \ddots & \ddots & \ddots & \ddots & \ddots \end{pmatrix}.$$

With an appropriate choice of the basis $\{u_\alpha(x)\}$ the matrix elements $(B)_{\alpha\beta}$ may couple only a finite number of basis functions. Then, the recurrence (24) would be solvable by continued fractions when the n-recurrence is infinite and this approach is seemingly precluded. Even for finite coupling in n, the α-recurrence may be preferable in certain situations (e.g., at low T), as indicated by Risken for a cosine potential in the classical limit ([14], section (11.5.6)). In these cases, one has been able to reduce the underlying large $(N \times A) \times (N \times A)$ problem to A problems with associated $N \times N$ matrices.

6. Density matrix, observables, and marginal distributions

Once the $\dot{\boldsymbol{c}}_n = \sum_m \mathbb{Q}_{nm}\boldsymbol{c}_m$ or $\dot{\boldsymbol{c}}_\alpha = \sum_\beta \mathbb{Q}_{\alpha\beta}\boldsymbol{c}_\beta$ are solved, we can reconstruct the Wigner function from its expansion coefficients C_n^α in the double basis $\{u_\alpha(x)\,\psi_n(p)\}$

$$W(x,p) = w(x,p)\sum_{n,\alpha} C_n^\alpha u_\alpha(x)\psi_n(p) \tag{26}$$

obtaining the *full solution of the quantum master equation*. If preferred, one can switch to the familiar density matrix $\hat{\varrho}$ by the inverse of transformation (1)

$$\varrho(x,x') = \int \mathrm{d}p\, \mathrm{e}^{\mathrm{i}p(x-x')/\hbar} W(\tfrac{1}{2}(x+x'),p). \tag{27}$$

We can get any observable inserting the above $W(x,p)$ in equation (2) for the averages. Nevertheless, common observables can many times be extracted *directly* from the C_n^α.

Let us illustrate this with transport observables, which are characterized by the averages $\langle p^\ell\rangle$. For an arbitrary function of p only, we get from (26)

$$\langle f\rangle = \int \mathrm{d}x\,\mathrm{d}p\, W(x,p) f(p) = \sum_{n,\alpha} C_n^\alpha \int \mathrm{d}x\, \mathrm{e}^{-\Phi(x)} u_\alpha(x) \int \mathrm{d}p\, r_0\, \mathrm{e}^{-\eta\, p^2/2} f(p)\psi_n(p), \tag{28}$$

where we have used $w = r_0\,\mathrm{e}^{-\eta\,p^2/2}\,\mathrm{e}^{-\Phi}$, with $r_0 = 1/(2\pi)^{1/4}$ (equations (9) and (10)). Next we introduce the auxiliary integrals (for their calculation see appendix D)

$$I_\alpha = \int \mathrm{d}x\, \mathrm{e}^{-\Phi(x)} u_\alpha(x), \qquad K_n^{(\ell)} = \int \mathrm{d}p\, r_0\, \mathrm{e}^{-\eta\, p^2/2} p^\ell \psi_n(p). \tag{29}$$

Then, the moments (case $f = p^\ell$) can be written in terms of the expansion coefficients as $\langle p^\ell\rangle = \sum_n K_n^{(\ell)} (\sum_\alpha C_n^\alpha I_\alpha)$. Taking into account that H_n has the parity of n and carrying this to $K_n^{(\ell)}$, we get for the first two

$$\langle p\rangle = \sum_n K_{2n+1}^{(1)} \Big(\sum_\alpha C_{2n+1}^\alpha I_\alpha\Big), \qquad \langle p^2\rangle = \sum_n K_{2n}^{(2)} \Big(\sum_\alpha C_{2n}^\alpha I_\alpha\Big). \tag{30}$$

The first moment is the *current* and the second characterizes *fluctuations* around it. The zeroth moment corresponds to the *normalization* of W, and imposes on the C_n^α the condition $\langle p^0\rangle = \sum_n K_{2n}^{(0)}(\sum_\alpha C_{2n}^\alpha I_\alpha) = 1$.

Finally, the quantum probabilities of x and p, given by the marginal distributions $P(x) = \int \mathrm{d}p\, W(x,p)$ and $P(p) = \int \mathrm{d}x\, W(x,p)$, can be expressed in a similar fashion

$$P(x) = \mathrm{e}^{-\Phi(x)} \sum_\alpha u_\alpha(x) \Big(\sum_n C_n^\alpha K_n^{(0)} \Big), \tag{31}$$

$$P(p) = r_0 \mathrm{e}^{-\eta\, p^2/2} \sum_n \psi_n(p) \Big(\sum_\alpha C_n^\alpha I_\alpha \Big). \tag{32}$$

7. Periodic potentials: matrix elements and limit cases

Henceforth, we shall apply the method described to incorporate fluctuations and dissipation in the problem of *quantum transport in periodic potentials*. The simplest model consists of a particle evolving in a cosine potential subjected to external forces (tilted 'washboard' potential), which is also a paradigm of *quantum Brownian motion* [45–47]. Others include potentials lacking inversion symmetry (ratchets), which have been used to model rectification of current and *directional motion* in several systems [48]. These problems are demanding because periodic potentials have (partly) continuous spectra [49], rendering inappropriate methods devised for systems with discrete levels. In this section we compute the matrix coefficients of our recurrences for arbitrary periodic $V(x)$. With them we can implement the continued-fraction method to solve the quantum master equation, which we first check by regaining the classical dissipative and quantum Hamiltonian limits.

7.1. Matrix elements

In periodic potentials the p-recurrence cannot be used because of its infinite coupling range (the derivatives of $V(x)$ neither vanish, nor decrease, as they are essentially the potential itself). However, one can guess that the x-recurrence may have a coupling range related to the number of harmonics in $V(x)$. To exploit this we introduce plane waves as basis functions and the Fourier expansion of the potential derivative:

$$u_\alpha(x) = \frac{\mathrm{e}^{\mathrm{i}\alpha x}}{\sqrt{2\pi}}, \qquad V'(x) = \sum_\alpha V'_\alpha\, \mathrm{e}^{\mathrm{i}\alpha x}. \tag{33}$$

To preserve the periodicity of W, one extracts the external force F from $V(x)$ including it in a generalized $D^\pm = d_\pm(\partial_x - \Phi') - \eta_\pm F$ (cf equation (15)). Then, the auxiliary potential Φ is set proportional to the periodic part $\Phi = \varepsilon V$.

To compute the matrix elements in $\mathbb{Q}_{\alpha\beta}$, we only need to do the integrals (20) with plane waves for u_α. Using $\partial_x u_\alpha = \mathrm{i}\alpha\, \mathrm{e}^{\mathrm{i}\alpha x}/\sqrt{2\pi}$, the integral $\int_0^{2\pi} \mathrm{d}x\, \mathrm{e}^{\mathrm{i}(\beta-\alpha)x} = 2\pi\delta_{\alpha\beta}$, and the expansion $V^{(s)} = \sum_r V_r^{(s)} \mathrm{e}^{\mathrm{i}rx}$, we find

$$(\partial_x)_{\alpha\beta} = \mathrm{i}\alpha\, \delta_{\alpha\beta}, \qquad [V^{(s)}(x)]_{\alpha\beta} = V^{(s)}_{\alpha-\beta}. \tag{34}$$

From these elements and $V_q^{(2s+1)} = (-1)^s q^{2s} V'_q$ we get

$$\begin{aligned} [\Gamma_n^{s,\pm} V^{(2s+1)}]_{\alpha\beta} &= 0 && \delta_{\alpha\beta} - \eta_\pm^{2s+1} G_n^s(-\sigma q^2 \lambda_{\mathrm{dB}}^2) && V'_{\alpha-\beta}, \\ D^\pm_{\alpha\beta} &= (\mathrm{i}d_\pm\alpha - \eta_\pm F) && \delta_{\alpha\beta} - d_\pm\varepsilon && V'_{\alpha-\beta} \end{aligned} \tag{35}$$

with $q=\alpha-\beta$, $m=n-(2s+1)$ and (cf equation (16))

$$G_n^s(z)=|\kappa_n^{(s)}(q)|\mathrm{e}^{-z/2}{}_1F_1(-m,2s+2;z),\qquad |\kappa_n^{(s)}(q)|=\frac{(q\lambda_{\mathrm{dB}})^{2s}}{(2s+1)!}\sqrt{\frac{n!}{m!}}. \tag{36}$$

That is, $\kappa_n^{(s)}(q)$ is the coefficient in (16) with $\lambda_{\mathrm{dB}}\to q\lambda_{\mathrm{dB}}$. Inserting equation (35) into the general matrices $\mathbb{Q}_{\alpha\beta}$ of section 5 we explicitly get the matrix coefficients of our recurrences (appendix E). For the cosine potential

$$V(x)=-V_0\cos x \tag{37}$$

the coupling range is 1, because $V_q'=0$ for $|q|>1$ and we have a three-term recurrence $\dot{\boldsymbol{c}}_\alpha=\mathbb{Q}_{\alpha,\alpha-1}\boldsymbol{c}_{\alpha-1}+\mathbb{Q}_{\alpha,\alpha}\boldsymbol{c}_\alpha+\mathbb{Q}_{\alpha,\alpha+1}\boldsymbol{c}_{\alpha+1}$. For a two-harmonic ratchet potential

$$V(x)=-V_0[\sin x+(r/2)\sin(2x)] \tag{38}$$

the range is 2 (five-term recurrence) because $V_q'=0$ for $|q|=|\alpha-\beta|>2$, and so on.

As we restricted $0\leqslant\eta\leqslant 1/2$, we have $\sigma=\eta_-\eta_+=\eta^2-1/4\leqslant 0$, so that $z=-\sigma q^2\lambda_{\mathrm{dB}}^2\geqslant 0$. Thus, the argument of G_n^s is positive and $\exp(-z/2)$ can act as a regularization factor (an advantage of allowing $\eta\neq 1/2$ in (10)). This factor reduces the weight of the off-diagonal terms inside $\mathbb{Q}_{\alpha\beta}$, enhancing the numerical stability when going into the deep quantum regime. Then we typically use $\eta\sim 0$–0.05, while for classical calculations $\eta=1/2$ performs better. Concerning the auxiliary potential Φ, for the problems considered below we use $\varepsilon=0$. Convergence is achieved with $N\sim 100$ Hermite functions and $A\sim 25$–50 plane waves (then $N\times(2A+1)\sim 10^4$). Finally, a word on the scaled quantities (section 3). To get period 2π, we have set $x_0=a/2\pi$ with a the original period. The characteristic energy E_0 is given by the potential amplitude $E_0=V_0$; then $k_{\mathrm{B}}T$ is scaled by V_0 and the other characteristic quantities are: action, $S_0=x_0\sqrt{MV_0}$, frequency, $\omega_0^2=V_0/Mx_0^2$, and force, $F_0=V_0/x_0$.

7.2. Classical limit

Before going into the quantum regime, let us check that for small enough $\hbar/S_0=2\pi/K$ we recover the classical results. Recall that in the deterministic limit a particle in a periodic potential has two critical forces F_1 (retrapping force) and F_3 (force at which the barrier disappears). For $F<F_1$ the attractors of the dynamical system are solutions 'locked' around the potential minima, whereas for $F>F_3$ the 'running' solution is an attractor globally stable. In the range $F_1<F<F_3$ the system exhibits bistability. Finally, F_1 decreases with γ (for the cosine potential $F_1\sim(4/\pi)V_0^{1/2}\gamma$), whereas F_1 tends to F_3 as the damping increases, narrowing the bistability range.

Thermal fluctuations are incorporated by the Klein–Kramers equation, which for classical particles in periodic potentials was solved by continued fractions in [14, 50–52] (using the p-recurrence). Here we solve the Caldeira–Leggett quantum master equation (4) using a large K. As shown before, when $V(x)=-V_0\cos(x)$ we have a three-term recurrence which, for the static response, can be written as

$$\mathbb{Q}_\alpha^-\boldsymbol{c}_{\alpha-1}+\mathbb{Q}_\alpha\boldsymbol{c}_\alpha+\mathbb{Q}_\alpha^+\boldsymbol{c}_{\alpha+1}=0 \tag{39}$$

with $\mathbb{Q}_\alpha^-=\mathbb{Q}_{\alpha,\alpha-1}$, $\mathbb{Q}_\alpha=\mathbb{Q}_{\alpha,\alpha}$, and $\mathbb{Q}_\alpha^+=\mathbb{Q}_{\alpha,\alpha+1}$. Solving it with the continued-fraction method we reobtain Risken's impressive graphs for the classical distribution $W(x,p)$ ([14], chapter 11.5). Some of them are displayed in figure 1 for weak damping and various external forces (here $F_1\simeq 0.064$ and $F_3=1$). At low F the distribution, always periodic along x, has maxima at the potential minima, while the profile in momenta is a Maxwellian envelope

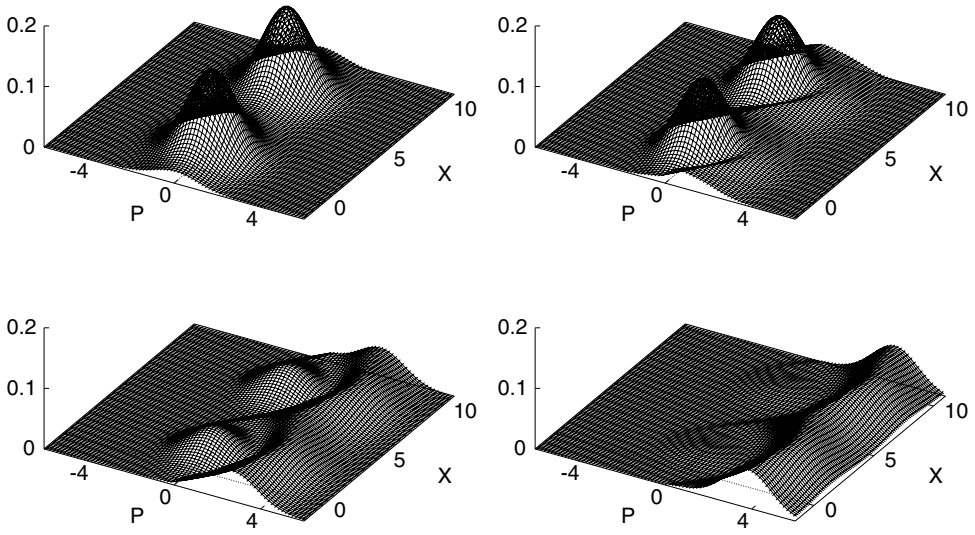

Figure 1. Wigner functions in the classical limit ($K = 1000$) for a particle in a tilted sinusoidal potential (two periods are displayed along x). Here $\gamma = 0.05$, and $T = 1$, while $F = 0$, 0.075, 0.15, and 0.2 (left to right, top to bottom).

$\sim \exp(-p^2/2)$. As F is increased we see the evolution from these *locked* solutions ($\langle p \rangle \simeq 0$) to bistability between the locked and *running* solutions, and eventually purely running states $W \sim \exp[-(p - F/\gamma)^2/2]$ are obtained at large forces.

7.3. Hamiltonian quantum case

7.3.1. Bands and quantum parameters. Having checked the retrieval of the classical results, we now enter the quantum regime by decreasing $K \sim S_0/\hbar$. Firstly, it will be useful to get a more quantitative feeling of the relation of our parameter K and 'how quantal is the system'. To this end we study the bands of the corresponding Hamiltonian problem (without force). Inserting the *Bloch* function $\Psi_{mq}(x) \propto \exp(\mathrm{i}qx)U_{mq}(x)$ in the Schrödinger equation, we arrive at the following eigenvalue problem (in scaled units; section 3):

$$\left[-\frac{1}{2}\left(\frac{2\pi}{K}\right)^2 (\mathrm{i}q + \partial_x)^2 + V(x)\right] U(x) = EU(x), \qquad -\tfrac{1}{2} \leqslant q \leqslant \tfrac{1}{2}. \tag{40}$$

Expanding $U(x)$ in plane waves (33) and truncating $|\alpha|$ at some large A one gets a $(2A+1) \times (2A+1)$ matrix which is diagonalized numerically. Various bands $E(q)$ pertaining to problems discussed below are displayed in figure 2. We see that the rule of thumb is that $K/2$ is of the order of the number of bands lying below the barrier. Finally, the quantum parameter used by Kandemir [53] is $(K/\pi)^2$, while Chen and Lebowitz employed $\Omega_q = \pi/K$ [54, 55]. Besides, for a Josephson junction problem we simply have $K = \pi(E_\mathrm{J}/2E_\mathrm{C})^{1/2}$, with E_J and E_C the Josephson and Coulomb energies.

7.3.2. Wignerian representation. Let us continue for a while in the Hamiltonian case to familiarize ourselves with the structure of the Schrödinger eigenstates in a phase-space representation. Kandemir [53] obtained analytical approximations for the eigenfunctions of a particle in a cosine potential in terms of Mathieu functions. They were represented through the

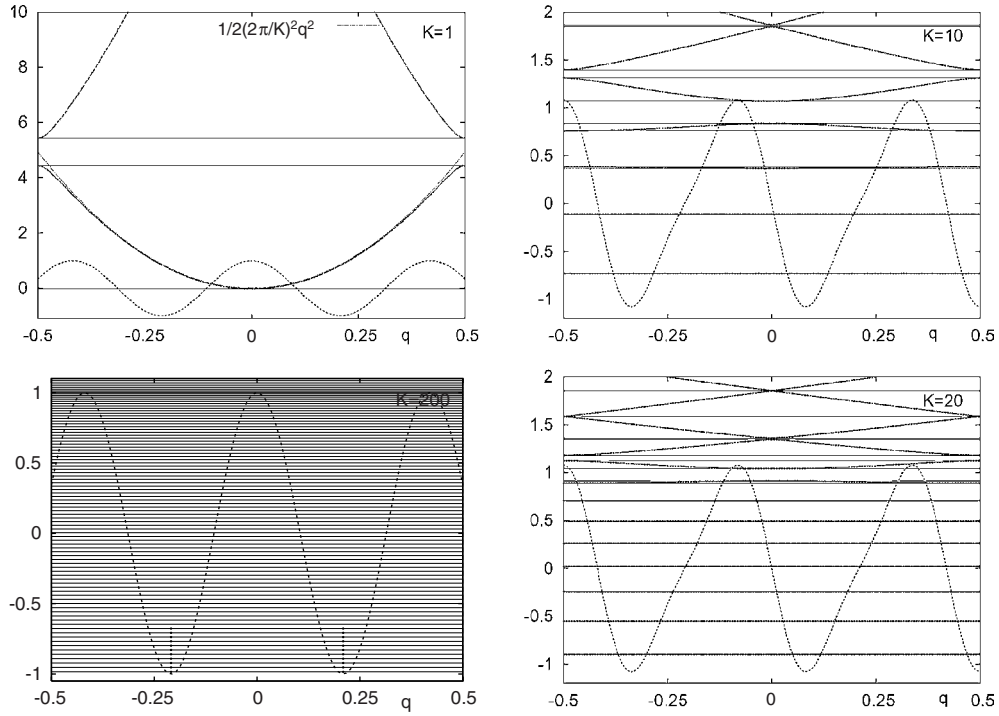

Figure 2. Energy bands for various K (reduced Kondo parameter (7)). The potential profile is plotted to show the number of bands below the barrier. Left panels: cosine potential for $K = 1$ (as in figures 3 and 4), with the free-particle parabolic relation $E \propto q^2$, and for $K = 200$ (figure 7), together with the first levels of the associated anharmonic oscillator (dots; equation (50)). Right panels: ratchet potential (38) with $r = 0.44$ for $K = 10$ and $K = 20$, as in figure 6.

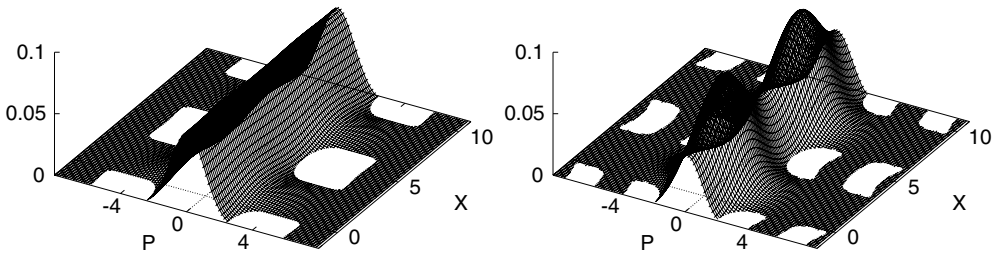

Figure 3. Wigner functions in the absence of dissipation for a particle in a sinusoidal potential (two periods are displayed). The reduced Kondo parameter is $K = 1$ (left) and 2 (right). The 'islands' correspond to zones of negative W.

Wigner function associated to the density matrix of pure states $\varrho(x, x') = \Psi(x)\Psi^*(x')$. (In [53] various Dirac deltas occurring were regularized with Gaussians $\delta(p) \sim (k/\pi)\exp(-k^2p^2)$ and in the plots $k = 1$ was used; we attain the same setting $T = 1$ since our p is thermally rescaled.)

Using a very small damping ($\gamma = 10^{-6}$) in the Caldeira–Leggett master equation we reobtain Kandemir's Hamiltonian results for the ground state (figure 3). We see that at low K the state is extended or delocalized, becoming more localized at the potential wells when $K \propto S_0/\hbar$ is increased. According to Kandemir [53], the regions of negative W are associated

to Brillouin zone boundaries. We have represented a larger range of p to see how these $W < 0$ islands are repeated in the p direction (W can be as small as $W \sim -10^{-9}$ bordering the limits of our numerical accuracy).

To see how these structures arise, note that for small K the potential can be treated perturbatively (equation (40)). Then, the wave functions have the form $\Psi_q(x) \propto e^{iqx}(1 + \lambda e^{+ix} + \lambda^* e^{-ix})$, with $\lambda = i(K/2\pi)^2$. The first term is a pure plane wave, and the rest first-order corrections due to the sinusoidal $V(x)$. Performing the Wigner transform (1) of this $\Psi_q(x)$, we get for the ground state $q = 0$ (cf [56], p 314)

$$W(x, p) = \delta(p) + |\lambda|^2[\delta(p-1) + \delta(p+1)] \\ -2|\lambda|^2 \cos(2x)\delta(p) + 2i\lambda \sin(x)[\delta(p - \tfrac{1}{2}) + \delta(p + \tfrac{1}{2})]. \qquad (41)$$

The first line gives the momentum localization at $p = 0$ (unperturbed) and at $p = \pm 1$. The first term in the second line arises from the interference of e^{+ix} and e^{-ix}, and is responsible for the weak modulation of the height of the $p = 0$ bell along x. This modulation is more intense for larger λ (i.e., larger K). The last term accounts for the interference between the plane wave centred at $p = 0$ with those at $p = \pm 1$, and can produce the negative islands. We therefore see that the above simple functional form captures most features of the Wigner functions of figure 3.

8. Periodic potentials: quantum dissipative case

Having checked the connection with the classical and Hamiltonian quantum limits, we finally include dissipation and temperature in the quantum case. Here examples of particles in cosine and ratchet potentials will be discussed.

8.1. Quantum Brownian motion in a cosine potential

Transport properties of weakly damped particles in a cosine potential were studied by Chen and Lebowitz [54, 55]. They started from the system-plus-bath density matrix, traced out the bath variables, and performed a perturbative calculation in the potential height (followed by a resummation) to get $\langle p \rangle$. For low forces a free-particle like behaviour $\langle p \rangle \propto F/\gamma$ was obtained. Increasing F, the wave vector associated to p approaches the first zone boundary (figure 2). There, while Landau–Zener tunnelling can bring the particle to the next band, Bragg scattering reduces the velocity ($\propto \partial E/\partial q$). Eventually, at larger forces, p corresponding to states inside the next band become favoured, and the free-particle behaviour is progressively recovered.

Since high $k_B T/\hbar\gamma$ approximations were involved in their calculations, we set $D_{pp} = \gamma M k_B T$ and $D_{xp} = 0$ in the master equation (4). Solving it with the continued-fraction method we reobtain the effect just described (figure 4; here we work in the regime $\hbar\gamma/k_B T \sim 0.1$). Note that the quantum slowing effect is reduced as γ increases, since the coupling to the bath 'broadens' the effective energy levels. This broadening makes the presence of the band gap less relevant ('bridges' it) and brings the curves progressively closer to the free-damped-particle behaviour $\langle p \rangle \propto F/\gamma$.

With our method we get, in addition, the Wigner function (i.e., the full density matrix). The distribution of velocities (32), $P(p) = \int dx\, W(x, p)$, when the curves start to rise again ($F/\gamma \sim 4.5$), shows two peaks separated by a minimum corresponding to the wave vector of the first zone boundary. Loosely speaking, the system shows coexistence of *two* quantum 'running' solutions. Classical running solutions have a wiggling structure along x, as the particle slows down near the potential maxima (figure 1). The full $W(x, p)$ shows that the quantum running solutions have a nearly straight structure (substrate insensitive). We also recognize the familiar

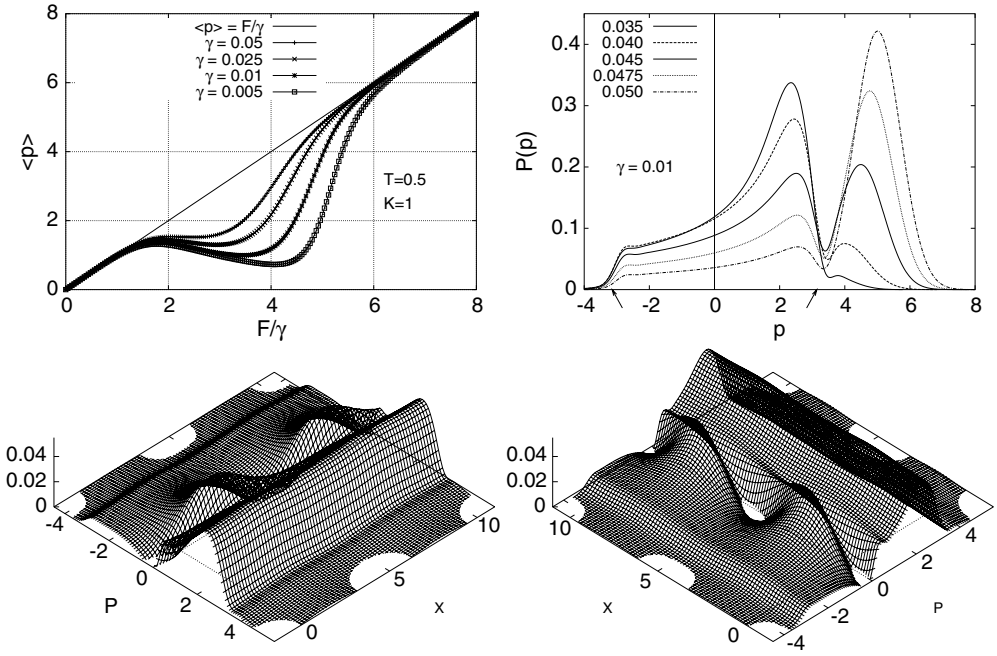

Figure 4. Upper panels. Left: $\langle p\rangle$ versus F for various dampings at $T = 0.5$ and $K = 1$. Right: marginal distribution of momenta $P(p) = \int \mathrm{d}x\, W(x, p)$ for $\gamma = 0.01$ at $F/\gamma = 3.5, 4, 4.5, 4.75$, and 5. The arrows mark the zone boundaries $|p| = \pi/K$. Lower panels: two views of $W(x, p)$ for $\gamma = 0.01$ and $F/\gamma = 3.5$.

crescent islands of negative W at large p (there $W \sim -0.0003$). Around $p \sim 0$ a complex structure is developed along x ('locked part'), with the maxima deformed and the minima becoming slightly negative ($W \sim -0.005$). These features may reflect some interference between the locked and the nearby running solution. However, simply adding a plane wave $\mathrm{e}^{+\mathrm{i}p_0 x}$ to the $\Psi_q(x)|_{q=0}$ used to analyse the Wigner functions of the Hamiltonian problem (equation (41)) we have not been able to reproduce such structure. In any case, it is erased when integrating over x to get $P(p)$.

8.2. Quantum Brownian motion in ratchet potentials

We now turn our attention to periodic potentials without spatial inversion symmetry. This feature combined with out-of-equilibrium conditions can give rise to directional motion with net unbiased driving (*ratchet effect*). This directional motion has been invoked to explain the behaviour of molecular motors and, with the emergence of nanoscience, opens the way to build mesoscopic devices and engines based on it. The theoretical work has concentrated on the classical behaviour and in the high-damping regime [48]. The few quantum studies also addressed strong system-bath coupling in two situations: semiclassical [57] and an extreme quantum case disregarding thermal effects [58]. An exception to the large γ studies is [59], but there the substrate potential (and the force) were treated perturbatively. Here, we shall solve the quantum master equation (4) with the (non-perturbative) continued-fraction method for particles in ratchet potentials, taking into account finite damping ($\sim$ non-negligible inertia).

For the ratchet potential (38), the Fourier coefficients of $V'(x)$ are $V'_{\pm 1} = -V_0/2k_\mathrm{B}T$ and $V'_{\pm 2} = -rV_0/2k_\mathrm{B}T$ (recall the thermal scaling of V; section 3). We use $r = 0.44$, which

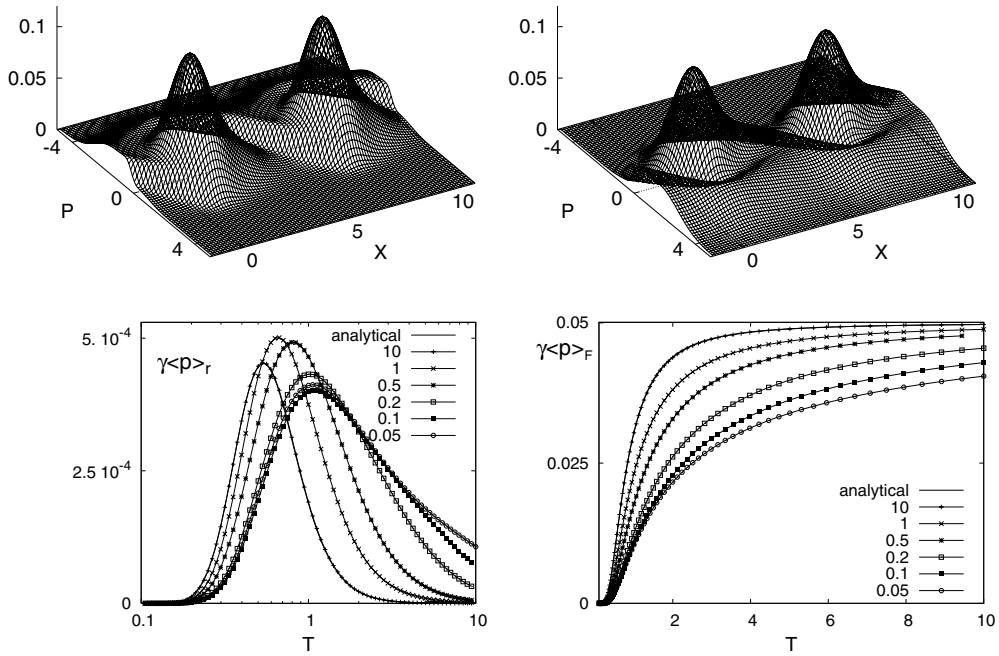

Figure 5. Upper panels: Wigner functions for a ratchet potential in the classical limit ($K = 1000$) with $\gamma = 0.05$ and $T = 1$. Two forces are used $F = -0.1$ (left) and $F = 0.1$ (right), to show the lack of symmetry in the response (running part more developed to the easy side) and the locked regions reflecting the potential profile. Lower left: Rectified classical velocity versus temperature for various values of the damping and force $|F| = 0.05$. Right: $\gamma\langle p\rangle$ versus T for the positive force.

smooths a small shoulder that this potential exhibits on the 'easy' side (figure 2). As discussed before, the range of index coupling is 2, which gives a five-term recurrence. For the stationary response it can be written as (cf equation (39))

$$\mathbb{Q}_\alpha^{--}\boldsymbol{c}_{\alpha-2} + \mathbb{Q}_\alpha^{-}\boldsymbol{c}_{\alpha-1} + \mathbb{Q}_\alpha\boldsymbol{c}_\alpha + \mathbb{Q}_\alpha^{+}\boldsymbol{c}_{\alpha+1} + \mathbb{Q}_\alpha^{++}\boldsymbol{c}_{\alpha+2} = 0, \tag{42}$$

which can be folded onto a canonical three-term recurrence by introducing appropriate (block) vectors and matrices (appendix A).

The potential considered is the minimal extension of the cosine potential lacking inversion symmetry, so that the average velocities can be different for positive and negative forces (see figure 5). We excite the system with a square-wave force switching alternatively between $\pm F$, and compute the 'rectified' current of particles

$$\gamma\langle p\rangle_{\mathrm{r}} = \gamma\langle p\rangle_{+F} + \gamma\langle p\rangle_{-F}. \tag{43}$$

Here $\langle p\rangle_{\pm F}$ are the corresponding stationary velocities since we consider adiabatic conditions ($\omega \to 0$). In what follows, we briefly investigate the classical limit (understudied for finite damping) and then proceed to study quantum corrections.

8.2.1. Classical case. Figure 5 displays $\langle p\rangle_{\mathrm{r}}$ as a function of T, showing the appearance of non-zero rectified velocities (ratchet effect). The rectification is optimum at some intermediate temperature (at too low T there is hardly a response, and at too high T the potential is irrelevant, so its asymmetry plays no role in either case). At $\gamma = 10$ the results coincide with those

obtainable from the analytical $\langle p\rangle$ for overdamped classical particles ([14], chapter 11.3) (see also [48, 60])

$$\gamma\langle p\rangle = \frac{2\pi T(1-\mathrm{e}^{-2\pi F/T})}{\int_0^{2\pi}\mathrm{d}x\,\mathrm{e}^{-\phi(x)}\int_0^{2\pi}\mathrm{d}y\,\mathrm{e}^{\phi(y)} - (1-\mathrm{e}^{-2\pi F/T})\int_0^{2\pi}\mathrm{d}x\,\mathrm{e}^{-\phi(x)}\int_0^{x}\mathrm{d}y\,\mathrm{e}^{\phi(y)}} \tag{44}$$

with $\phi(x) = [V(x) - Fx]/T$. Inertia, however, broadens the $\langle p\rangle_{\mathrm{r}}$ curves and shifts the maxima to higher T (for the lowest $\gamma = 0.05$ the maximum moves to a slightly lower T; see below). This broadening is accompanied by a slower decrease of $\langle p\rangle_{\mathrm{r}}$ with T. This is consistent with the asymptotic behaviour of $\langle p\rangle_{\mathrm{r}}$ when $T \to \infty$ [59]. For overdamped particles it goes as $\langle p\rangle_{\mathrm{r}} \sim T^{-4}$, while for weak damping it decreases only with $\langle p\rangle_{\mathrm{r}} \sim T^{-(17/6)}$ ($17/6 \lesssim 3$). We have checked that our results recover these functional dependences (curves not shown due to the smallness of the asymptotic $\langle p\rangle_{\mathrm{r}} \sim 10^{-6}$–$10^{-7}$).

In our case $F \lesssim \gamma \sim F_1$ (the 'retrapping' force; section 7.2), so that at $T = 0$ the attractors are locked solutions. Then, the absolute $\gamma\langle p\rangle$ versus T curves start from $\langle p\rangle = 0$ at $T = 0$, depart from zero as T is increased and evolve towards $\gamma\langle p\rangle = F$ for $T \to \infty$ (free damped particle). In the overdamped case this evolution is nearly a step, whereas the slope of the initial raising decreases with decreasing γ (if $F < F_1$). To understand this, let us assimilate $\langle p\rangle$ to the escape rate Γ (modified by some mean free path), so that $\gamma\langle p\rangle \sim \gamma\Gamma$. Kramers' [61] theory shows that $\gamma\Gamma$ increases monotonously with γ. Therefore, the $\gamma\langle p\rangle$ versus T curves for finite γ must lie ordered below the overdamped result. On the other hand, the maximum rectification occurs in the temperature region where $\gamma\langle p\rangle$ transits from 0 to F. This intermediate region is narrower (and the slopes steeper) the higher the damping is (figure 5), while the curves start to raise from zero at a lower T. Therefore, increasing the damping the $\gamma\langle p\rangle_{\mathrm{r}}$ curves will be narrower and the maxima shift to lower T, as observed. Eventually, this also allows to explain the anomalous curve showing the return ($\gamma = 0.05$). Here $\gamma \sim F$, so that at $T = 0$ the system starts close to the zone of bistability. Then the particle can perform incursions into the running solution, increasing the initial slope of $\gamma\langle p\rangle_{\pm F}$ but now when the damping is lowered, shifting the maximum to a lower T.

8.2.2. Quantum corrections. After the mandatory exploration of the classical limit, we proceed to make the system quantal by decreasing K. Figure 6 shows the rectified current with $K = 15$ (with seven bands below the barrier; cf figure 2) for various γ, together with the reference classical curves. We have set $|F|/\gamma = 1$ in all cases, to have roughly the same amount of locked and running components in the solutions. At high temperatures ($k_{\mathrm{B}}T \gg V_0$) the classical and quantum curves coincide, as expected. However, decreasing T down to $k_{\mathrm{B}}T \sim V_0$, the ratchet effect gets reduced or enhanced, with respect to the classical result, depending on the dissipation. Finally, at low temperatures ($k_{\mathrm{B}}T \ll V_0$) the rectification is always reduced.

To understand qualitatively the underlying physics, we turn to some semiclassical results for various related problems. Firstly, let us consider the *reflection/transmission coefficient* for an asymmetric saw-tooth potential ([62], sections 50, 52). The results depend on the energy of the incident quantum particle. The reflection coefficient for energies higher than the barrier, $\mathcal{R}$, and the underbarrier transmission coefficient, $\mathcal{T}$, read

$$\mathcal{R} = \frac{\hbar^2/2M}{(4E)^3}(f_2 - f_1)^2, \qquad \mathcal{T} = \exp\left[-\frac{2}{\hbar}\left|\int_a^b \mathrm{d}x\; p(x)\right|\right] \tag{45}$$

where f_1, f_2 are the slopes at both sides of the cusp, E the particle energy, and $p(x) = \sqrt{2M[E - V(x)]}$. Suppose now that we have an asymmetric potential, with an easy direction to the right, and we deform it with forces $\pm F$, computing the corresponding reflection coefficients

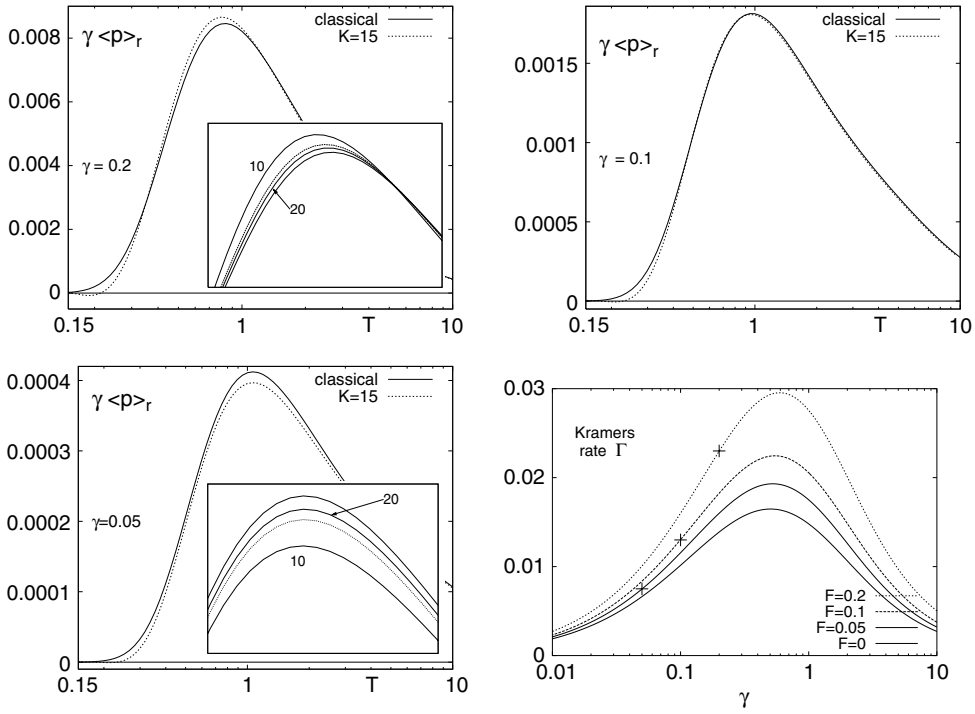

Figure 6. Rectified velocity versus T with $\gamma = 0.2, 0.1, 0.05$ (using $|F|/\gamma = 1$) for $K = 15$ and the reference classical curve ($K = 1000$). The insets of $\gamma = 0.2$ and 0.05 show enlargements of the peaks (together with results for $K = 20$ and 10). Lower right panel: Kramers classical rate versus γ at various forces (from Mel'nikov–Meshkov formula [61]). The crosses mark the points with $F/\gamma = 1$.

$\mathcal{R}_+$ and $\mathcal{R}_-$. For energies higher than the barrier, the above $\mathcal{R}$ gives $\mathcal{R}_+/\mathcal{R}_- < 1$ (appendix F). That is, *overbarrier wave reflection* is less intense when the slope of the potential is smaller. Thus overbarrier transmission (as thermal hopping) is favoured along the easy direction for energies above the barrier [63]. In contrast, using $\mathcal{T}$ for energies below the barrier, we find $\mathcal{T}_+/\mathcal{T}_- < 1$, so that $\mathcal{R}_+/\mathcal{R}_- > 1$. That is, the reflection is more intense in the easy direction or, equivalently, tunnelling events are favoured in the hard direction [57].

For a distribution of particle energies one would expect a competition between these two types of quantum effects. Then, the enhancement of the rectified velocity under $\pm F$ forcing for the $\gamma = 0.2$ curve follows from the increase of the thermal escape with γ in the intermediate-to-low damping range $\gamma \leqslant 0.5$ (figure 6). At that damping, more escape events occur and the particles launched over the barrier are subjected to the discussed phenomenon of wave reflection, which favours net motion along the easy side and hence increases $\langle p \rangle_{\mathrm{r}}$. Lowering the damping, on the other hand, fewer escape events are produced and wave reflection becomes progressively dominated by tunnel events (favouring the hard direction). Incidentally, at $k_{\mathrm{B}}T \sim V_0$ one would expect the tunnel to be thermally assisted through the higher bands, which are wider. A simple estimation of channel probabilities comes from multiplying a band thermal population (using Kramers' rate) by the probability of tunnel (given by the semiclassical transmission coefficient $\mathcal{T}$). Here the exponential reduction of Γ with E competes with the exponential increase of $\mathcal{T}$ for the upper bands (appendix F). At $k_{\mathrm{B}}T \sim V_0$ and for $K = 15$ we find that tunnel is indeed favoured through the upper bands.

To check that the behaviours found at the maxima are systematic, we increase K to 20 (nine bands below the barrier) and reduce it to $K = 10$ (four bands; here the temperatures around the peak are still inside the range of validity of the master equation, small $\hbar\gamma/k_{\rm B}T$). The results (insets) show clearly the tendency to amplify either the enhancement or the reduction when the system becomes more quantal.

Finally, at low temperatures ($k_{\rm B}T \sim V_0/5$) thermal activation becomes inefficient for all dampings. Then a reduction of the rectification is expected, due to dominance of below-barrier energies and hence of tunnel events (through the lowest bands). Note that the decrease in $\langle p\rangle_{\rm r}$ relative to the classical results is comparable in the curves shown. This suggests that we have similar crossover temperatures T_0 in this damping range. (T_0, below which quantum effects dominate, is useful as a measure of quantum corrections at a given T.) This quantity is known exactly in the problem of the escape from a 'quadratic-plus-cubic' potential $V(x) = \frac{1}{2}M\omega_0^2x^2[1-(2x/3x_0)]$ ([7], chapter 14)

$$T_0 = (\hbar\omega_0/2\pi k_{\rm B})(\sqrt{1+a^2}-a), \qquad a = \gamma/2\omega_0. \tag{46}$$

In our units $T_0 \to (\sqrt{1+\gamma^2/4}-\gamma/2)/K$ and in the damping range studied the factor in brackets is close to 1 ($\sim 0.9, 0.95, 0.975$). This gives crossovers $T_0 \sim 1/K \sim 0.07$ and hence comparable reductions of the ratchet effect, as observed. This reduction of the rectification is the precursor of the current reversals ($\langle p\rangle_{\rm r} < 0$) found in these systems when tunnelling completely dominates. Although we find small $\langle p\rangle_{\rm r} < 0$ in some cases, the results cannot be fully trusted. For example, at $\gamma = 0.2$, $K = 15$ and $T = 0.2$, we have $\hbar\gamma/k_{\rm B}T \sim 0.5$, which is bordering the limits of validity of the quantum master equation employed here.

9. Periodic potentials: dynamic response

We conclude with the study of the (non-adiabatic) dynamic response to oscillating forces $F(t) = \Delta F\cos(\omega t)$. Then, the coefficients of the expansion (26) of the Wigner function are periodic functions of t, so they can be Fourier-expanded as follows:

$$C(t) = C^{(0)} + \sum_{k=1}^{\infty}\left(\frac{\Delta F}{2}\right)^k (C^{(k)}{\rm e}^{+{\rm i}k\omega t} + C^{(-k)}{\rm e}^{-{\rm i}k\omega t}). \tag{47}$$

To lowest order in the probing field, the static part of the corresponding vectors (equation (24)) obeys a recurrence relation of the type (see appendix G)

$$\mathbb{Q}_\alpha^- \boldsymbol{c}_{\alpha-1}^{(0)} + \mathbb{Q}_\alpha \boldsymbol{c}_\alpha^{(0)} + \mathbb{Q}_\alpha^+ \boldsymbol{c}_{\alpha+1}^{(0)} = 0. \tag{48}$$

The equations for the harmonics have the form ($\mathbb{I}$ is the identity matrix)

$$\mathbb{Q}_\alpha^- \boldsymbol{c}_{\alpha-1}^{(k)} + ({\rm i}k\omega\mathbb{I} + \mathbb{Q}_\alpha)\boldsymbol{c}_\alpha^{(k)} + \mathbb{Q}_\alpha^+ \boldsymbol{c}_{\alpha+1}^{(k)} = -\boldsymbol{f}_\alpha \tag{49}$$

with the 'forcing' $\boldsymbol{f}_\alpha$ involving the previous order results. Specifically, $\boldsymbol{f}_\alpha \sim \Delta\mathbb{Q}_\alpha \boldsymbol{c}_\alpha^{(k-1)}$, with $\Delta\mathbb{Q}_\alpha$ the part of $\mathbb{Q}_\alpha$ corresponding to ΔF, namely

$$\Delta\mathbb{Q}_\alpha = \begin{pmatrix} 0 & \sqrt{1}\eta_+\Delta F & 0 & 0 & \ddots \\ \sqrt{1}\eta_-\Delta F & 0 & \sqrt{2}\eta_+\Delta F & 0 & \ddots \\ 0 & \sqrt{2}\eta_-\Delta F & 0 & \sqrt{3}\eta_+\Delta F & \ddots \\ 0 & 0 & \sqrt{3}\eta_-\Delta F & 0 & \ddots \\ \ddots & \ddots & \ddots & \ddots & \ddots \end{pmatrix}$$

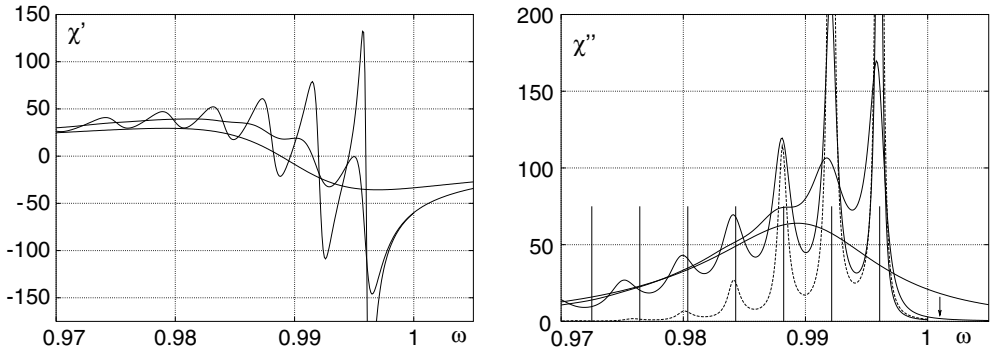

Figure 7. Linear dynamical susceptibility versus frequency at $T = 0.05$ and $K = 200$ with $\gamma = 0.01$ ($\sim$ classical), 0.0003 and 0.0001 (less to more peaked curves). Left panel: real part. Right panel: imaginary part (dashed line, $\gamma = 0.0001$ but halving $T = 0.025$). Vertical lines: loci of the transition frequencies of the associated quadratic plus quartic anharmonic oscillator (equation (51)).

(see appendix E for the general $\mathbb{Q}_{\alpha\beta}$; the $\Delta\mathbb{Q}_\alpha$ actually entering in $\boldsymbol{f}_\alpha$ is divided by ΔF, cf equations (G.1) and (G.4)). Equations (48) and (49) can be solved sequentially with the continued-fraction method (first $k = 0$, then $k = 1$, etc).

Figure 7 shows the linear susceptibility ($k = 1$) computed in this way for a particle in a *cosine* potential as a function of ω. (Here we return to safe ground because $\hbar\gamma/k_BT \sim 10^{-2}$–$10^{-4}$; for related dielectric and Kerr relaxation curves of a quantum rotator see [64] and references therein.) For the largest damping the results correspond to the classical limit. There the line-shape $\chi''(\omega)$ broadens and extends to frequencies lower than the oscillation frequency near the bottom of the potential wells ($\omega/\omega_0 = 1$ in our units). For low damping, this classical *spreading of oscillation frequencies* has an important contribution from the amplitude dependence of the period of oscillation in anharmonic potentials [14, 50]. This non-dissipative contribution to $\chi''(\omega)$ is also known in classical spin problems, where the precession frequency depends on S_z due to the magnetic anisotropy [65, 66].

The quantum regime is approached by decreasing the Kondo parameter $\alpha \sim \gamma K$ (equation (7)). Reducing γ with a fixed K we find that the $\chi(\omega)$ curves develop a multipeaked structure. These peaks could be vaguely seen as the mentioned nonlinear oscillations becoming quantized. To give content to this statement, we investigate perturbatively the effect of the anharmonic terms of a cosine potential (those beyond $\propto x^2$) on the energy levels of the harmonic oscillator part. Since the main contribution should come from the quartic term, we consider the potential $V(x) = \frac{1}{2}M\omega_0^2x^2 + bx^4$. First-order perturbation theory gives the eigenvalues ([67], chapter 6.3)

$$E_m \simeq \hbar\omega_0(m + \tfrac{1}{2}) + 3b(\hbar/2M\omega_0)^2(2m^2 + 2m + 1). \tag{50}$$

Expanding the cosine potential $V(x) = -V_0\cos(x/x_0)$, we identify $M\omega_0^2 = V_0/x_0^2$ and $b = -V_0/(x_0^4\,4!)$ (<0, soft anharmonicity). Then we can compute the level spacing

$$\Delta E_{m+1,m} = \hbar\omega_0\left[1 - \frac{\hbar(m+1)}{8M\omega_0x_0^2}\right], \tag{51}$$

which has acquired a dependence on the level index m absent in the harmonic case. The associated transition frequencies $E_{m+1,m}/\hbar$ are plotted in figure 7 (scaled as $\omega_{m+1,m}/\omega_0 = 1 - \pi(m+1)/4K$). They agree well with the location of the main peaks of the quantum

$\chi''(\omega)$ curves, supporting their relation with the nonlinearity of the potential. Furthermore, the contribution from transitions between the higher levels should be reduced when they are less populated. Decreasing T, we indeed see that the corresponding peaks (located at lower ω) are substantially reduced. In the suggestive language of nonlinear oscillations, we would say that lowering the temperature the large-amplitude oscillations (having longer period) become less probable.

The applicability of the quantum nonlinear oscillator picture is grounded on the flatness of the lowest bands at the K considered, which are well approximated by constant levels (see figure 2). We have computed the semiclassical width of the bands in a cosine potential in appendix F. An upper bound for the width (equation (F.9)) reads in dimensionless units as $W_{\rm b} = (4/K)\exp[-\frac{1}{2}K(1-\varepsilon)]$, with $\varepsilon = E/V_0$ the band mean energy relative to the potential amplitude. For moderate K this bound gives in fact very flat bands, specially the deepest ones ($E \to -V_0$). This also implies that the width of the $\chi''(\omega)$ peaks has a negligible contribution from the intrinsic level width, being dominated by the damping and thermal broadening.

10. Discussion

Traditionally, the continued-fraction method has been employed to solve Fokker–Planck equations for few-variable classical systems (translational and rotational problems). When compared with numerical simulations of the Langevin equation, the method has several *shortcomings*: (i) it is quite specific to the problem to be solved (one needs to recalculate the recurrence coefficients for each potential), (ii) its convergence and stability depend on the parameters of the problem (and can be poor in some ranges) and (iii) it does not return 'trajectories', which in the simulations provide helpful insight. Nevertheless, when the method can be used, its *advantages* are most valuable: (i) it is free from statistical errors, (ii) it is essentially nonperturbative, (iii) it is especially apt to get stationary solutions (static and dynamic), (iv) it has high efficiency (allowing one to explore parameter ranges out of the reach of the simulation) and (v) it gives the distribution W, which certainly compensates for the lack of trajectories.

For these reasons, and the lack of quantum Langevin simulations, it was worth developing continued-fraction methods for quantum dissipative systems. This had been done for problems of spins in a thermal bath and in quantum nonlinear optics. In this paper, we have discussed in detail the adaptation of the continued-fraction method to tackle quantum master equations in phase-space problems, taking advantage of the parallels with the classical case provided by the Wigner formalism. We have seen that the quantum extension of the continued-fraction method is more problem-dependent (except for polynomial potentials), due to the necessity of using the x-recurrence of the quantum hierarchies and finding suitable bases. Nevertheless, it inherits from the classical methods most of the above-mentioned advantages, in particular, obtaining the Wigner function, from which any observable can be computed. Furthermore, the eigenvalue spectrum of the system, although helpful in understanding the physics, is not necessarily required. This is advantageous when dealing with non-bounded Hamiltonians, continuous spectra, etc. Finally, by changing the appropriate quantum parameter, the connection with the classical results is attained in a natural way.

Note that 'continued-fraction' is a quite generic term (like 'series expansion'), which can be found in many different contexts, and in particular in works dealing with quantum dissipative systems (see, e.g., [68] and references therein). However, in those cases one usually obtains some continued-fraction expression for a certain quantity (e.g., the linear susceptibility, memory functions, etc), whereas we have obtained the *complete solution of the quantum master equation* by continued-fraction methods. The approach allows us to study the interplay of

quantum phenomena, nonlinearity, thermal fluctuations, and dissipation in several classes of systems. This is important, because methods optimized for one of the sides (e.g., nonlinearity or quantal behaviour) tend to perform poorly for the others (e.g., fluctuations or dissipation). In addition, the visualization of $W(x, p)$ plus the knowledge of the classical phase-space structure (orbits, separatrices, attractors, etc) can provide valuable insight in difficult problems. Finally, the main limitations of the approach are those that the starting master equations may have. We have considered the celebrated Caldeira–Leggett quantum master equation, but the method can be applied to a class of equations of this type, and to possible generalizations.

We have implemented the method in the canonical problem of quantum Brownian motion in periodic potentials. We have considered both the cosine and the ratchet potentials. For the former, we have recovered and extended a number of classic results and interpreted them on the basis of the Wigner formalism. Results for the dynamics under oscillating forcing have also been obtained, illustrating the modification of the nonlinear effect of spreading of oscillation frequencies by quantum phenomena. For particles in ratchet potentials we have studied, under adiabatic conditions, the effects of finite damping on the rectified velocity. Taking into account the competition of thermal hopping, overbarrier wave reflection and tunnel events, together with semiclassical analytical results, has allowed us to understand in great detail the physics of these systems.

Acknowledgments

This work was supported by DGES (project BFM2002-00113) and DGA (grant no. B059/2003). We acknowledge F Falo, J J Mazo and A P Piazzolla for useful discussions and valuable inspiration.

Appendix A. Solving recurrence relations by continued fractions

Here we briefly discuss the solution of recurrence relations by continued-fraction methods. We first consider three-term recurrences and then differential recurrences, vector-matrix cases, folding of larger-coupling recursions into three-term ones, and the problem of the initial conditions. (For a brief description of the relation of continued fractions, series expansions, recursions and orthogonal polynomials see [69].)

Suppose we have the simplest case of a three-term recurrence relation of the form

$$Q_i^- C_{i-1} + Q_i C_i + Q_i^+ C_{i+1} = -f_i, \qquad i = 0, \pm 1, \pm 2, \ldots \tag{A.1}$$

with Q_i and f_i given quantities. To obtain the C_i one inserts into (A.1) the ansatz [14, 70] (upper and lower signs for $i > 0$ and $i < 0$)

$$C_i = S_i C_{i\mp 1} + a_i \tag{A.2}$$

obtaining the following ladder coefficients S_i and shifts a_i:

$$S_i = -\frac{Q_i^{\mp}}{Q_i + Q_i^{\pm} S_{i\pm 1}}, \qquad a_i = -\frac{f_i + Q_i^{\pm} a_{i\pm 1}}{Q_i + Q_i^{\pm} S_{i\pm 1}}. \tag{A.3}$$

If the recurrence is finite or the C_i decrease quickly with $|i|$ (e.g., when they are coefficients of some judiciously chosen expansion), we can truncate at some large $|i| = I$, by setting $S_{\pm I} = 0$ and $a_{\pm I} = 0$. Next we *iterate downwards* in (A.3) getting S_i and a_i, down to $i = 0$. Then, to get the C_i from (A.2), we need C_0, which is obtained from

$$(Q_0^- S_{-1} + Q_0 + Q_0^+ S_1) C_0 = -(f_0 + Q_0^- a_{-1} + Q_0^+ a_1), \tag{A.4}$$

combination of equation (A.1) at $i = 0$ and $C_{\pm 1} = S_{\pm 1} C_0 + a_{\pm 1}$. Thus, starting from C_0, we *iterate* $C_i = S_i C_{i\mp 1} + a_i$ *upwards*, getting the solution of the recursion. For $f_i \equiv 0$ (homogeneous recurrences), we have $a_i = 0$ and the solution reads $C_i^{(\mathrm{h})} = S_i S_{i-1} \cdots S_1 C_0^{(\mathrm{h})}$. Note that S_i is given in terms of S_{i+1} in the denominator, which can in turn be written as a fraction with S_{i+2} in the denominator, and so on. This has the structure of a *continued fraction*, naming the method

$$C = \cfrac{p_1}{q_1 + \cfrac{p_2}{q_2 + \cdots}}. \tag{A.5}$$

The iterative solution can be cast into explicit form as a series of products of continued fractions [71]. The above form, however, has the virtue of being easy to implement in a computer. Convergence is checked by increasing $I \to 2I \to \cdots$ and by repeating the procedure. Solving equation (A.1) in this way requires a computational effort of order I, instead of the order I^2 of an arbitrary linear algebra problem. This reduction arises from the tridiagonal structure of the matrix associated to (A.1). (For analytical inversion of tridiagonal matrices see [72] and references therein.)

We can solve analogously a differential recurrence of the type

$$\mathrm{d}C_i/\mathrm{d}t = Q_i^- C_{i-1} + Q_i C_i + Q_i^+ C_{i+1} + f_i. \tag{A.6}$$

Laplace transformation converts this equation into $[\tilde{g}(s) \equiv \int_0^\infty \mathrm{d}t\, \mathrm{e}^{-st} g(t)]$

$$Q_i^- \widetilde{C}_{i-1} + (Q_i - s)\widetilde{C}_i + Q_i^+ \widetilde{C}_{i+1} = -[\tilde{f}_i + C_i(0)], \tag{A.7}$$

where $\tilde{\tilde{g}}(s) = s\,\tilde{g}(s) - g(0)$ has been used. Then, introducing $Q_i' = Q_i - s$ and $f_i' = \tilde{f}_i + C_i(0)$, the above equation has the structure of the ordinary recurrence (A.1).

The quantities involved in the above recurrences need not to be scalars, but they can be J-vectors (C_i and f_i) and the coefficients Q_i are $J \times J$ matrices. Then we speak of *matrix continued fractions*. The only change in the above solution is that the fraction bars then mean matrix inversion ('from the left', $A/B \to B^{-1} A$).

This is important because a recurrence relation involving more than three coefficients can be 'folded' into a three-term recurrence by introducing vector and matrix quantities. Let us show how to do so for the following five-term recursion:

$$Q_i^{--} C_{i-2} + Q_i^- C_{i-1} + Q_i C_i + Q_i^+ C_{i+1} + Q_i^{++} C_{i+2} = -f_i. \tag{A.8}$$

Defining the 2-vectors

$$\boldsymbol{c}_i = \begin{pmatrix} C_{2i} \\ C_{2i+1} \end{pmatrix} \qquad \text{and} \qquad \boldsymbol{f}_i = \begin{pmatrix} f_{2i} \\ f_{2i+1} \end{pmatrix}$$

and the 2×2 matrices

$$\mathbb{Q}_i^- = \begin{pmatrix} Q_{2i}^{--} & Q_{2i}^- \\ 0 & Q_{2i+1}^{--} \end{pmatrix} \qquad \mathbb{Q}_i = \begin{pmatrix} Q_{2i} & Q_{2i}^+ \\ Q_{2i+1}^- & Q_{2i+1} \end{pmatrix} \qquad \mathbb{Q}_i^+ = \begin{pmatrix} Q_{2i}^{++} & 0 \\ Q_{2i+1}^+ & Q_{2i+1}^{++} \end{pmatrix},$$

it can be easily seen that equation (A.8) for $2i$ and $2i + 1$ is equivalent to

$$\mathbb{Q}_i^- \boldsymbol{c}_{i-1} + \mathbb{Q}_i \boldsymbol{c}_i + \mathbb{Q}_i^+ \boldsymbol{c}_{i+1} = -\boldsymbol{f}_i. \tag{A.9}$$

Then, insertion of $\boldsymbol{c}_i = \mathbb{S}_i \boldsymbol{c}_{i\mp 1} + \boldsymbol{a}_i$ gives the matrix version of (A.3). Note that the C_i and f_i can already be vectors and the Q_i matrices. Then, the above $\boldsymbol{c}_i$, $\boldsymbol{f}_i$ and $\mathbb{Q}_i$ are 'block' vectors and matrices.

Finally, to iterate upwards $\boldsymbol{c}_i = \mathbb{S}_i \boldsymbol{c}_{i\mp1} + \boldsymbol{a}_i$, the 'initial condition' $\boldsymbol{c}_0$ is obtained from the matrix version of (A.4) (which we write $\mathbb{A}\mathbf{x} = \mathbf{b}$). As in the absence of forcing ($\boldsymbol{f}_i = 0$) the general solution involves an overall multiplicative constant, one adds to this system an extra equation to fix it (e.g., a normalization condition on the coefficients; section 6). Alternatively, we can fix arbitrarily one element of $\boldsymbol{c}_0$ and rescale the solution at the end. In either case, one has an extra equation which added to $\mathbb{A}\,\mathbf{x} = \mathbf{b}$ yields the extended $(J+1) \times J$ system

$$\mathbb{A}^*\mathbf{x} = \mathbf{b}^*, \qquad \mathbb{A}^* = \left(\begin{array}{c} \overleftarrow{\quad J \quad}\overrightarrow{\quad} \\ \hline \mathbb{A} \\ \hline \text{lhs equation} \end{array}\right) \begin{array}{c} \uparrow \\ (J+1) \\ \downarrow \end{array} \quad \mathbf{b}^* = \left(\begin{array}{c} b_1 \\ \vdots \\ b_J \\ \hline \text{rhs} \end{array}\right) \tag{A.10}$$

This system can be solved by any method appropriate for cases with more equations than unknowns (e.g., using QR or SVD decomposition [73]), obtaining $\boldsymbol{c}_0$.

Appendix B. Derivation of the transformed evolution operator $\overline{\mathcal{L}}$

Here we derive $\overline{\mathcal{L}}$, the $w^{-1}(\cdot)w$ transform of the operator $\mathcal{L}$ in the master equation with $w \propto \exp[-(\eta\, p^2/2 + \Phi)]$ (equation (10)). We split $\overline{\mathcal{L}}$ as $\overline{\mathcal{L}} = \overline{\mathcal{L}}_{\rm ir} + \overline{\mathcal{L}}_{\rm kin} + \overline{\mathcal{L}}_{\rm v}$, with $\mathcal{L}_{\rm ir}$, $\mathcal{L}_{\rm kin}$, and $\mathcal{L}_{\rm v}$ given by (8). For the 'product' of operators we use that the transformation of the product is equal to the product of the transformations:

$$\overline{AB} = \overline{A}\;\overline{B}, \qquad \overline{A^m} = (\overline{A})^m \tag{B.1}$$

which follows by sandwiching 'identities' $ww^{-1} = 1$ between the factors. Besides, the multiplication by functions of (x, p) commutes with $w^{-1}(\,\cdot\,)w$, so that only the differential terms need to be transformed. From these two properties we see that *only $\overline{\partial_x}$ and $\overline{\partial_p}$ need to be calculated* (and then raised to some power or multiplied).

B.1. Calculation of $\overline{\partial_x}$ and $\overline{\partial_p}$

Calculation of $\overline{\partial_x}$. In order to transform ∂_x, we apply $w^{-1}\partial_x w$, to an arbitrary function $f(x, p)$. The p dependent part of w cancels out and we obtain

$$\overline{\partial_x} f = \mathrm{e}^{\Phi}(-\partial_x\Phi\,\mathrm{e}^{-\Phi} f + \mathrm{e}^{-\Phi}\partial_x f), \qquad \rightsquigarrow \qquad \overline{\partial_x} = \partial_x - \Phi', \tag{B.2}$$

which has the form of a 'displaced' differential operator.

Calculation of $\overline{\partial_p}$. Applying $w^{-1}\partial_p w$ to a function f, we similarly get $\overline{\partial_p}$:

$$\overline{\partial_p} f = \mathrm{e}^{\eta\, p^2/2}(-\eta p\,\mathrm{e}^{-\eta\, p^2/2} f + \mathrm{e}^{-\eta\, p^2/2}\partial_p f), \qquad \rightsquigarrow \qquad \overline{\partial_p} = \partial_p - \eta\, p. \tag{B.3}$$

This $\overline{\partial_p}$ can be expressed in terms of the following creation and annihilation operators:

$$b = \partial_p + \tfrac{1}{2}p, \qquad b^+ = -\partial_p + \tfrac{1}{2}p. \tag{B.4}$$

Thus, using the shifted η parameters $\eta_\pm = \eta \mp \frac{1}{2}$ (equation (14)) we arrive at

$$\overline{\partial_p} = -(\eta_- b^+ + \eta_+ b). \tag{B.5}$$

For $\eta = 1/2$ (the choice in the classical case), $\eta_- = 1$ and $\eta_+ = 0$, so that $\overline{\partial_p} = -b^+$.

B.2. Calculation of $\overline{\mathcal{L}_{\rm ir}} = w^{-1}\mathcal{L}_{\rm ir}w$

Using the product property $\overline{A\,B} = \overline{A}\,\overline{B}$, we have $\overline{\mathcal{L}_{\rm ir}} = \gamma_T\overline{\partial_p}(p + \overline{\partial_p})$. Then, replacing ∂_p by its 'bar' form (B.5) and writing $p = b + b^+$ (from (B.4)), we find

$$-\gamma_T^{-1}\overline{\mathcal{L}_{\rm ir}} = \eta_+(1-\eta_-) + \eta_-(1-\eta_-)b^+b^+ + 2(\eta - \eta_-\eta_+)b^+b + \eta_+(1-\eta_+)bb.$$

Here we have also used $\eta_- + \eta_+ = 2\eta$ and the commutation rule $[b, b^+] = 1$ to get a *normally ordered* form. If we introduce some compact notation for the coefficients

$$\gamma_{\rm d} = 2\gamma_T(\eta - \eta_-\eta_+), \qquad \gamma_- = \gamma_T\eta_-(1-\eta_-),$$
$$\gamma_{+-} = \gamma_T\eta_+(1-\eta_-), \qquad \gamma_+ = \gamma_T\eta_+(1-\eta_+),$$

we can finally write

$$\overline{\mathcal{L}_{\rm ir}} = -(\gamma_{+-} + \gamma_- b^+b^+ + \gamma_{\rm d}b^+b + \gamma_+ bb). \tag{B.6}$$

(The choice $\eta = 1/2$ gives the self-adjoint form $\overline{\mathcal{L}_{\rm ir}} = -\gamma_T\, b^+b$ [14].)

B.3. Calculation of $\overline{\mathcal{L}_{\rm kin}} = w^{-1}\mathcal{L}_{\rm kin}w$

Using equations (B.2) and (B.5) for $\overline{\partial_x}$ and $\overline{\partial_p}$, as well as $p = b + b^+$ and the definition (15) of $d_\pm$ we get for the kinetic part $\overline{\mathcal{L}_{\rm kin}} = -(p - D_{xp}\overline{\partial_p})\,\overline{\partial_x}$:

$$\overline{\mathcal{L}_{\rm kin}} = -bd_+(\partial_x - \Phi') - b^+d_-(\partial_x - \Phi').$$

The coefficients of b and b^+ are D^- and D^+, also defined in (15), and we have

$$\overline{\mathcal{L}_{\rm kin}} = -(bD^+ + b^+D^-). \tag{B.7}$$

B.4. Calculation of $\overline{\mathcal{L}_{\rm v}} = w^{-1}\mathcal{L}_{\rm v}w$

To obtain $\overline{\mathcal{L}_{\rm v}} = \sum_{s\geqslant 0}\kappa^{(s)}V^{(2s+1)}\overline{\partial_p^{(2s+1)}}$ (see equation (8)), we use the product property (B.1) to raise $\overline{\partial_p}$ to $2s+1$, obtaining

$$\overline{\mathcal{L}_{\rm v}} = -\sum_{s\geqslant 0}\kappa^{(s)}V^{(2s+1)}(\eta_-b^+ + \eta_+b)^{2s+1}. \tag{B.8}$$

To obtain later the matrix elements of $\overline{\mathcal{L}_{\rm v}}$ between Hermite functions, it is convenient to cast (B.8) in a normally ordered form. To this end we use Pathak's theorems [74] in the following generalized form:

$$\frac{(a^+ + a)^{2s+1}}{(2s+1)!} = \sum_{q=0}^{s}\frac{{:}(a^+ + a)^{2(s-q)+1}{:}}{[2(s-q)+1]!}\frac{(\sigma/2)^q}{q!}. \tag{B.9}$$

Here ${:}(a^+ + a)^m{:} = \sum_{k=0}^m c_k^m(a^+)^{m-k}a^k$ with $c_k^m \equiv m!/[k!\,(m-k)!]$ (${:}f{:}$ is the result of moving the a^+ to the left as if they were scalars). The generalization resides in letting a and a^+ have a constant but different from one commutator. In our case

$$a = \eta_+b, \qquad a^+ = \eta_-b^+, \qquad \rightsquigarrow \qquad [a, a^+] = \sigma \tag{B.10}$$

follows from the commutator $[b, b^+] = 1$ with $\sigma = \eta_-\eta_+$. Note that a and a^+ are not the adjoint of each other, but the notation is symbolic.

With the help of equation (B.9) and $\kappa^{(s)} = (-1)^s\lambda_{\rm dB}^{2s}/(2s+1)!$ (equation (6)) we can write (B.8) as follows:

$$\overline{\mathcal{L}_{\rm v}} = -\sum_{s=0}^{\infty}\sum_{q=0}^{s}A_{s,q}\hat{X}^{2(s-q)+1}, \tag{B.11}$$

where we have introduced the notations

$$A_{s,q} = \frac{(-1)^s \lambda_{\rm dB}^{2s}}{[2(s-q)+1]!} \frac{(\sigma/2)^q}{q!} V^{(2s+1)}, \qquad \hat{X}^\ell = {:}(a^+ + a)^\ell{:}.$$

For a given s different powers of $\hat{X}$ appear. We take a common factor $\hat{X}^\ell$ and add coefficients, e.g., $A_{00} + A_{11} + A_{22} + \cdots$ with $\hat{X}$, $A_{10} + A_{21} + A_{32} + \cdots$, with $\hat{X}^3$, etc

$$\sum_{s=0}^{\infty} \sum_{q=0}^{s} A_{s,q} \hat{X}^{2(s-q)+1} = \sum_{\ell=0}^{\infty} \left(\sum_{s=\ell}^{\infty} A_{s,s-\ell} \right) \hat{X}^{2\ell+1} = \sum_{\ell=0}^{\infty} \left(\sum_{q=0}^{\infty} A_{q+\ell,q} \right) \hat{X}^{2\ell+1}.$$

For $s = q + \ell$ in $A_{s,q}$ we write $V^{[2(q+\ell)+1]} = \partial_x^{2q} V^{(2\ell+1)}$ and introduce the operator Δ

$$A_{q+\ell,q} = \frac{(-\Delta/2)^q}{q!} \frac{(-1)^\ell \lambda_{\rm dB}^{2\ell}}{(2\ell+1)!} V^{(2\ell+1)}, \qquad \Delta = \sigma \lambda_{\rm dB}^2 \partial_x^2. \tag{B.12}$$

Now the q and ℓ dependences factorize, so we can sum the series of q in $E_\ell \equiv \sum_{q=0}^{\infty} A_{q+\ell,q}$, getting an exponential. Then, recalling the definition of $\kappa^{(s)}$ we finally obtain the normally ordered form for $\overline{\mathcal{L}}_{\rm v}$ we were looking for

$$\overline{\mathcal{L}}_{\rm v} = -\sum_{\ell=0}^{\infty} E_\ell {:}(a^+ + a)^{2\ell+1}{:}, \qquad E_\ell = \kappa^{(\ell)} \exp(-\Delta/2) V^{(2\ell+1)}. \tag{B.13}$$

The operator $\exp(-\Delta/2)$ does not act on what could appear after $V(x)$, since Δ was introduced as some abbreviated notation for the high-order derivatives of the potential.

Appendix C. The different contributions to $\partial_t C_n = \sum_m \hat{Q}_{nm} C_m$

Here we calculate the matrix elements $\hat{Q}_{nm} = \int \mathrm{d}p\, \psi_n \overline{\mathcal{L}}\, \psi_m$, with the transformed operator $\overline{\mathcal{L}} = \overline{\mathcal{L}}_{\rm ir} + \overline{\mathcal{L}}_{\rm kin} + \overline{\mathcal{L}}_{\rm v}$ obtained in appendix B. We split in parts the calculation by introducing the corresponding decomposition: $\hat{Q}_{nm}^{\rm ir} = \langle n|\overline{\mathcal{L}}_{\rm ir}|m\rangle$, $\hat{Q}_{nm}^{\rm kin} = \langle n|\overline{\mathcal{L}}_{\rm kin}|m\rangle$ and $\hat{Q}_{nm}^{\rm v} = \langle n|\overline{\mathcal{L}}_{\rm v}|m\rangle$, where we have used the custom 'bra'–'ket' notation. The calculation is simplified because we have all operators $\overline{\mathcal{L}}$ expressed as normally ordered forms of b and b^+. Then we can take advantage of the ladder actions $b^+|n\rangle = \sqrt{n+1}\,|n+1\rangle$, $b\,|n\rangle = \sqrt{n}\,|n-1\rangle$, and the number property $b^+ b\,|n\rangle = n\,|n\rangle$.

C.1. Calculation of $\sum_m \hat{Q}_{nm}^{\rm ir} C_m$

From (B.6) for $\overline{\mathcal{L}}_{\rm ir}$ and the orthonormality of the $|m\rangle$, we find for $\hat{Q}_{nm}^{\rm ir} = \langle n|\overline{\mathcal{L}}_{\rm ir}|m\rangle$

$$-\hat{Q}_{nm}^{\rm ir} = \gamma_- \sqrt{(n-1)n}\,\delta_{n-2,m} + (n\gamma_{\rm d} + \gamma_{+-})\delta_{nm} + \gamma_+ \sqrt{(n+1)(n+2)}\,\delta_{n+2,m}.$$

Then, we introduce the notation $\gamma_n = n\,\gamma_{\rm d} + \gamma_{+-}$ for the coefficient of the diagonal term (cf equation (13)), multiply by C_m and sum over m, obtaining

$$-\sum_m \hat{Q}_{nm}^{\rm ir} C_m = \gamma_- \sqrt{(n-1)n}\, C_{n-2} + \gamma_n C_n + \gamma_+ \sqrt{(n+1)(n+2)}\, C_{n+2}. \tag{C.1}$$

C.2. Calculation of $\sum_m \hat{Q}^{\rm kin}_{nm} C_m$

Using equation (B.7) for $\overline{\mathcal{L}}_{\rm kin}$ and the 'ladder' action of b and b^+, we have

$$\hat{Q}^{\rm kin}_{nm} = -\langle n|bD^+ + b^+D^-|m\rangle = -(\sqrt{n+1}\ D^+\delta_{n+1,m} + \sqrt{n}\ D^-\delta_{n-1,m}),$$

where we have used the Kronecker delta to interchange n and $m \mp 1$. Then, multiplying by C_m and summing over m, one obtains

$$\sum_m \hat{Q}^{\rm kin}_{nm} C_m = -(\sqrt{n} D^- C_{n-1} + \sqrt{n+1} D^+ C_{n+1}). \tag{C.2}$$

C.3. Calculation of $\sum_m \hat{Q}^{\rm v}_{nm} C_m$

This calculation is more tedious. Firstly, the operator $:(a^+ + a)^{2\ell+1}:$ appearing in equation (B.10) for $\overline{\mathcal{L}}_{\rm v}$ can be put in explicit form by using the binomial formula

$$:(a^+ + a)^{2\ell+1}: = \sum_{k=0}^{2\ell+1} c_k^{2\ell+1} (a^+)^{2\ell+1-k} a^k. \tag{C.3}$$

The a and a^+ are proportional to b and b^+ (equation (B.10)), so the contribution of each summand to $\langle n|\overline{\mathcal{L}}_{\rm v}|m\rangle$ involves $\langle n|(b^+)^{2\ell+1-k} b^k|m\rangle \propto \langle n-(2\ell+1)+k|m-k\rangle$. From orthonormality only one term of the sum (C.3) will contribute, namely $2k = (m-n)+2\ell+1$, while $m-n$ will be odd, $m = n \mp (2s+1)$ with $s \geqslant 0$ (reflecting the odd powers of ∂_p in $\mathcal{L}_{\rm v}$). Then, in terms of s, the index k is restricted to

$$k = \begin{cases} \ell - s, & \text{for } m = n-(2s+1), \\ \ell + s + 1, & \text{for } m = n+(2s+1). \end{cases} \tag{C.4}$$

Relating the results for $m = n \mp (2s+1)$. The two cases can be easily related. Firstly, the combinatorial coefficients are equal $c^{2\ell+1}_{\ell+s+1} = c^{2\ell+1}_{\ell-s}$, because $c^m_k = c^m_{m-k}$. Secondly, the η factors, coming from the proportionality of the a, a^+, to b, b^+, are simply obtained from each other by exchanging plus and minus symbols ($\sigma = \eta_-\eta_+$):

$$\begin{aligned} k = \ell - s \qquad &\rightsquigarrow \qquad \eta_-^{\ell+s+1}\eta_+^{\ell-s} = \sigma^{\ell-s}\eta_-^{2s+1}, \\ k = \ell + s + 1 \qquad &\rightsquigarrow \qquad \eta_-^{\ell-s}\eta_+^{\ell+s+1} = \sigma^{\ell-s}\eta_+^{2s+1}. \end{aligned} \tag{C.5}$$

Finally, the matrix elements are also relatable. For $m = n-(2s+1)$, we have $\langle n|(b^+)^{\ell+s+1} b^{\ell-s}|n-(2s+1)\rangle$, while for $m = n+(2s+1)$

$$\langle n|(b^+)^{\ell-s} b^{\ell+s+1}|n+(2s+1)\rangle = \langle m|(b^+)^{\ell+s+1} b^{\ell-s}|m-(2s+1)\rangle,$$

which is formally identical to the former by replacing $n \to n' = m$ and $m \to m' = n$.

Thus, from now onwards, we consider only the case $m = n-(2s+1)$ (factor $\sigma^{\ell-s}\eta_-^{2s+1}$). The result for $m = n+(2s+1)$, will be readily obtained from this by replacing

$$n' = m, \quad m' = n'-(2s+1) \quad \text{and} \quad \eta_-^{2s+1} \to \eta_+^{2s+1}. \tag{C.6}$$

From all these considerations, we can write the matrix elements of $:(a^+ + a)^{2\ell+1}:$ as

$$\langle n|:(a^+ + a)^{2\ell+1}:|m\rangle = \eta_-^{2s+1} c^{2\ell+1}_{\ell-s} \sigma^{\ell-s} \langle n|(b^+)^{\ell+s+1} b^{\ell-s}|m\rangle$$

where we omit a Kronecker delta ensuring $m = n-(2s+1)$. The rest of the calculation consists of multiplying this by E_ℓ and sum over all ℓ to get $\langle n|\overline{\mathcal{L}}_{\rm v}|m\rangle$ (equation (B.13)).

Restrictions on the sum on ℓ. The contribution of the infinite sum (B.13) to $\langle n|\overline{\mathcal{L}}_{\rm v}|m\rangle$ is fortunately cut-off. Firstly, the lower index in $c_{\ell-s}^{2\ell+1}$ should be positive and, introducing the shifted index $\ell' = \ell - s$, we obtain (we rename $\ell' \to \ell$ at the end)

$$\langle n|\overline{\mathcal{L}}_{\rm v}|m\rangle = -\eta_-^{2s+1}\sum_{\ell=0}^{m} E_{\ell+s}c_\ell^{2(\ell+s)+1}\sigma^\ell\langle n|(b^+)^{(2s+1)+\ell}b^\ell|m\rangle. \tag{C.7}$$

Here we have already used that the sum is also cut-off from above at $\ell_{\max} = m$, since $b^\ell|m\rangle \equiv 0$, for $\ell > m$. On the other hand, for $E_{\ell+s}$ (equation (B.13)) we have

$$E_{\ell+s} = {\rm e}^{-\Delta/2}\frac{(2s+1)!}{[2(\ell+s)+1]!}(-\lambda_{\rm dB}^2\partial_x^2)^\ell\frac{(-1)^s\lambda_{\rm dB}^{2s}}{(2s+1)!}V^{(2s+1)}. \tag{C.8}$$

Combining this with $c_\ell^{2(\ell+s)+1}$, gathering $(\lambda_{\rm dB}^2\partial_x^2)^\ell$ with σ^ℓ to form the operator Δ (equation (B.12)), and recalling definition (6) of $\kappa^{(s)}$, we obtain

$$\langle n|\overline{\mathcal{L}}_{\rm v}|m\rangle = -\eta_-^{2s+1}\kappa^{(s)}{\rm e}^{-\Delta/2}\sum_{\ell=0}^{m}\frac{(2s+1)!}{[(2s+1)+\ell]!}\langle n|(b^+)^{(2s+1)+\ell}b^\ell|m\rangle\frac{(-\Delta)^\ell}{\ell!}V^{(2s+1)}.$$

Note that the quotient of factorials equals $1/(2s+2)_\ell$, with the Pochhammer symbol defined by ([37], chapter 13.5)

$$(a)_\ell = a(a+1)\cdots(a+\ell-1) = (a+\ell-1)!/(a-1)!. \tag{C.9}$$

Computation of the matrix element. To conclude, we only need the matrix element $\langle n|(b^+)^{(2s+1)+\ell}b^\ell|m\rangle$ in (C.7). We first pass $2s+1$ times the action of b^+ to $|n\rangle$ by taking its adjoint b and then we use repeatedly its downward ladder action, obtaining

$$b^{2s+1}|n\rangle = \sqrt{n(n-1)\cdots(n-2s)}\,|n-(2s+1)\rangle = \sqrt{n!/m!}|m\rangle \tag{C.10}$$

with $m = n-(2s+1)$. Then, in terms of the Pochhammer symbol (C.9), we can write

$$\langle n|(b^+)^{(2s+1)+\ell}b^\ell|m\rangle = \sqrt{n!/m!}\langle m|(b^+)^\ell b^\ell|m\rangle = \sqrt{n!/m!}(-1)^\ell(-m)_\ell.$$

Now, taking into account that the factor $(-1)^\ell$ cancels that of $(-\Delta)^\ell$ and using the modified coefficient $\kappa_n^{(s)} = \kappa^{(s)}\sqrt{n!/m!}$ (equation (16)), we arrive at

$$\langle n|\overline{\mathcal{L}}_{\rm v}|m\rangle = -\eta_-^{2s+1}\kappa_n^{(s)}\,{\rm e}^{-\Delta/2}\left[\sum_{\ell=0}^{m}\frac{(-m)_\ell}{(2s+2)_\ell}\frac{\Delta^\ell}{\ell!}\right]V^{(2s+1)}.$$

Comparing this with the series definition of the confluent hypergeometric (Kummer) function ${}_1F_1(a,c;z)$ ([37], chapter 13.6) we obtain

$$\langle n|\overline{\mathcal{L}}_{\rm v}|m\rangle = -\eta_-^{2s+1}\kappa_n^{(s)}[{\rm e}^{-\Delta/2}\,{}_1F_1(-m,2s+2;\Delta)]V^{(2s+1)} \qquad {}_1F_1(a,c;z) = \sum_{\ell=0}^{\infty}\frac{(a)_\ell}{(c)_\ell}\frac{z^\ell}{\ell!}.$$

The operator in front of $V(x)$ is simply $\Gamma_n^{s,-}$ (equation (16)), so that we can finally write

$$\hat{Q}_{nm}^{\rm v} = \langle n|\overline{\mathcal{L}}_{\rm v}|m\rangle = -\Gamma_n^{s,-}V^{(2s+1)}(x), \qquad m = n-(2s+1). \tag{C.11}$$

Note that ${}_1F_1(-m,2s+2;z)$ is a polynomial because the first negative index cuts the upper Pochhammer symbol. Indeed the 'integer-plus-one' second argument $(2s+1)+1$ tells us that it is an associated Laguerre polynomial ([37], chapter 13)

$$L_\ell^k(z) = \frac{(\ell+k)!}{k!\ell!}\,{}_1F_1(-\ell,k+1;z). \tag{C.12}$$

In our case $\ell = m$ and $k = n-m = 2s+1$, so that ${}_1F_1(-m,2s+2;z) = L_m^{2s+1}(z)/c_n^m$.

Final expressions for $\sum_m \hat{Q}^{\rm v}_{nm}C_m$. Once we have computed $\hat{Q}^{\rm v}_{nm}$, the matrix elements of $\overline{\mathcal{L}}_{\rm v}$, we multiply by C_m and sum over m (i.e., over s), to get

$$\sum_{m<n}\hat{Q}^{\rm v}_{nm}C_m = -\sum_{s\geqslant 0}[\Gamma^{s,-}_n V^{(2s+1)}]C_{n-(2s+1)}.$$

Note that this s-sum is restricted because $n-(2s+1)\geqslant 0$. This yields the upper limit $s_{\max}=[(n-1)/2]$, with $[a]$ the integer part of a. The contribution from $m>n$ is easily obtained recalling the transformation rules (C.6) (here the sum is not restricted)

$$\sum_{m>n}\hat{Q}^{\rm v}_{nm}C_m = -\sum_{s\geqslant 0}[\Gamma^{s,+}_{n+(2s+1)} V^{(2s+1)}]C_{n+(2s+1)}$$

with $\Gamma^{s,+}_n$ given by (16). We have enclosed in square brackets the action of the operators $\Gamma^{s,\pm}_n$ to recall that they only act on the x-dependence of the potential.

For $\eta=1/2$, the choice in the classical case, $\eta_-=1$, $\eta_+=0$, and $\sigma=0$. Then, $\Gamma^{s,-}_n(\sigma=0)=\kappa^{(s)}_n$ and $\Gamma^{s,+}_n(\sigma=0)=0$, so that only the $C_{n-(2s+1)}$ terms survive. The chain of equations then aquires an unbalanced structure (like in the old hierarchies [38, 40, 41]), which may result in a poor stability when the quantum terms are important. In contrast, $\eta\sim 0$ gives $|\eta_\pm|\sim 1/2$, and hence the weight of the terms at both sides of n is similar ($\sim$ above and below the diagonals in the matrices $\mathbb{Q}_{\alpha\beta}$), improving the stability when going into the deep quantum regime.

Appendix D. The auxiliary integrals I_α and $K^{(\ell)}_n$

For special η and Φ, the integrals I_α and $K^{(\ell)}_n$ (equation (29)) appearing in the expressions (30) for the observables, are easily done. For $\eta=1/2$, we simply have $K^{(0)}_n=\delta_{n,0}$, $K^{(1)}_n=\delta_{n,1}$, and $K^{(2)}_n=\delta_{n,0}+\sqrt{2}\,\delta_{n,2}$. If $\Phi=0$ (i.e., $\varepsilon=0$), we get $I_\alpha=I_0\delta_{\alpha,0}$. Then the first moments reduce to $1=I_0C^0_0$ (normalization) and to $\langle p\rangle=I_0C^0_1$ and $\langle p^2\rangle=I_0(C^0_0+\sqrt{2}C^0_2)$. In the general case, one can derive recurrences relating the $K^{(\ell)}_n$ with lower order (in ℓ) ones. Thus, only $K^{(0)}_n$ is needed, which can be found analytically. Concerning the I_α, we mostly use $\varepsilon=0$, and hence $I_\alpha=I_0\delta_{\alpha,0}$. In any case, for periodic potentials one can derive recurrence relations for them which can also be solved by continued fractions.

D.1. The integrals $K^{(\ell)}_n$ (arbitrary potentials)

To obtain the recurrence for the $K^{(\ell)}_n$ we start from their definition (29) with index $\ell+1$, express the last p as $p=b+b^+$ (equation (B.4)), and then use $p\psi_n=\sqrt{n}\psi_{n-1}+\sqrt{n+1}\psi_{n+1}$, obtaining

$$K^{(\ell+1)}_n=\sqrt{n}K^{(\ell)}_{n-1}+\sqrt{n+1}K^{(\ell)}_{n+1}. \tag{D.1}$$

This recurrence can be used to get the $K^{(\ell+1)}_n$ from the $K^{(\ell)}_n$.

We can get analytical expressions for the first few $K^{(\ell)}_n$ with help from the tabulated integral ([75], equation (7.374-4))

$$\int_{-\infty}^{\infty}{\rm d}x\,{\rm e}^{-x^2}H_m(x)H_{2n+m}(ax)=\sqrt{\pi}\frac{(2n+m)!}{n!}(2a)^m(a^2-1)^n. \tag{D.2}$$

For $K^{(0)}_n=r_0\int {\rm e}^{-\eta p^2/2}\psi_n$, we use this result with $m=0$, obtaining

$$K^{(0)}_{2n+1}=0,\qquad K^{(0)}_{2n}=\frac{\sqrt{(2n)!}}{n!}\eta_-^{-1/2}\Lambda^n,\qquad \Lambda=-\eta_+/2\eta_-. \tag{D.3}$$

Although $K_n^{(1)}$ and $K_n^{(2)}$ can now be obtained from (D.1), they can also be done from equation (D.2), obtaining $K_{2n}^{(1)} = 0$, $K_{2n+1}^{(2)} = 0$, and

$$K_{2n+1}^{(1)} = \frac{\sqrt{(2n+1)!}}{n!}\frac{1}{\eta_-^{3/2}}\Lambda^n, \qquad K_{2n}^{(2)} = \frac{\sqrt{(2n)!}}{n!}\frac{1}{\eta_-^{3/2}}\left(\frac{n}{\eta_-}+\Lambda\right)\Lambda^{n-1}. \tag{D.4}$$

D.2. Recursions for the integrals I_α (periodic potentials)

For a general periodic potential we can derive a recurrence relation for the integrals $I_\alpha = \int_0^{2\pi} \mathrm{d}x \exp[-\varepsilon V(x)] u_\alpha(x)$ (equation (29)). We integrate by parts the expression for $\mathrm{i}\alpha I_\alpha$ and use $V' = \sum_\alpha V'_\alpha \mathrm{e}^{\mathrm{i}\alpha x}$ with $u_\alpha = \mathrm{e}^{\mathrm{i}\alpha x}/\sqrt{2\pi}$, obtaining

$$\mathrm{i}\alpha I_\alpha = \varepsilon \sum_\beta V'_\beta I_{\alpha+\beta}. \tag{D.5}$$

For a finite number of harmonics ($V'_\beta \equiv 0$, if $|\beta| > B$), the recurrence (D.6) has a finite coupling range. For instance, for the ratchet potential (38), we have $V'_{\pm 1} = -V_0/2k_\mathrm{B}T$ and $V'_{\pm 2} = -rV_0/2k_\mathrm{B}T$ and the above recurrence reduces to

$$\mathrm{i}\alpha I_\alpha = -\varepsilon_T[(I_{\alpha-1} + I_{\alpha+1}) + r(I_{\alpha-2} + I_{\alpha+2})], \qquad \varepsilon_T = \varepsilon V_0/2k_\mathrm{B}T. \tag{D.6}$$

With I_0 as input (obtained numerically, e.g., by the Simpson rule ([37], appendix 2)), this recursion can be solved by continued fractions (appendix A).

Appendix E. The matrices $\mathbb{Q}_{\alpha\beta}$ for general periodic potentials

Here we write explicitly the matrices $\mathbb{Q}_{\alpha\beta}$ for arbitrary periodic potentials. We shall give the results for a slightly generalized basis, obtained by shifting the origin of momenta by an amount ρ (cf equation (26)):

$$W(x,p) = w(x, p-\rho)\sum_{n,\alpha} C_n^\alpha u_\alpha(x)\psi_n(p-\rho). \tag{E.1}$$

This momentum shift is convenient to 'catch' solutions centred far from zero p, where the ordinary basis would need many $\psi_n(p)$ to reconstruct the distribution. (A useful choice is, when generating a curve, to set $\rho = \langle p\rangle$ of the precedent point.) The momentum shift is handled as a change of variable $p \to p_\rho = p - \rho$. Then, $\partial_p = \partial_{p_\rho}$, but the term $p\partial_x$ makes the force to enter in the combination (scaled units)

$$F_\rho = F - \gamma_T \rho. \tag{E.2}$$

As mentioned in section 7, we extract the force F from $V(x)$ and set the auxiliary potential Φ proportional to the periodic part $\Phi = \varepsilon V$.

The $\mathbb{Q}_{\alpha\beta}$ are obtained by inserting the formulae for $D^\pm_{\alpha\beta}$, and $[\Gamma_n^{s,\pm} V^{(2s+1)}]_{\alpha\beta}$ (equation (35)), into the general matrices of section 5. Instead of giving a single expression, we write separately the matrices for $\beta = \alpha$ and $\beta = \alpha \pm q$. The central matrix $\mathbb{Q}_{\alpha\alpha}$ is determined by the terms involving $\delta_{\alpha\beta}$, and reads

$$-\mathbb{Q}_{\alpha\alpha} = \begin{pmatrix}
\gamma_0+\rho\,\mathrm{i}\alpha & \sqrt{1}(\mathrm{i}d_+\alpha - \eta_+ F_\rho) & \sqrt{1\cdot 2}\,\gamma_+ & 0 & 0 & \ddots \\
\sqrt{1}(\mathrm{i}d_-\alpha - \eta_- F_\rho) & \gamma_1+\rho\,\mathrm{i}\alpha & \sqrt{2}(\mathrm{i}d_+\alpha - \eta_+ F_\rho) & \sqrt{2\cdot 3}\,\gamma_+ & 0 & \ddots \\
\sqrt{1\cdot 2}\,\gamma_- & \sqrt{2}(\mathrm{i}d_-\alpha - \eta_- F_\rho) & \gamma_2+\rho\,\mathrm{i}\alpha & \sqrt{3}(\mathrm{i}d_+\alpha - \eta_+ F_\rho) & \sqrt{3\cdot 4}\,\gamma_+ & \ddots \\
0 & \sqrt{2\cdot 3}\,\gamma_- & \sqrt{3}(\mathrm{i}d_-\alpha - \eta_- F_\rho) & \gamma_3+\rho\,\mathrm{i}\alpha & \sqrt{4}(\mathrm{i}d_+\alpha - \eta_+ F_\rho) & \ddots \\
0 & 0 & \sqrt{3\cdot 4}\,\gamma_- & \sqrt{4}(\mathrm{i}d_-\alpha - \eta_- F_\rho) & \gamma_4+\rho\,\mathrm{i}\alpha & \ddots \\
\ddots & \ddots & \ddots & \ddots & \ddots & \ddots
\end{pmatrix}$$

with $\gamma_\pm$ and γ_n given by (13), $\eta_\pm = \eta \mp 1/2$, and $d_\pm = 1 + \eta_\pm D_{xp}$. Here the periodic potential does not appear; only F enters in the matrices $\mathbb{Q}_{\alpha\alpha}$. Besides, they do depend on the index α (cf below).

The matrices $\mathbb{Q}_{\alpha,\alpha\pm q}$ are determined by the terms involving $V'_{\alpha-\beta}$ in equation (35) and read

$$-\mathbb{Q}_{\alpha,\alpha\pm q} = V'_{\mp q}\begin{pmatrix} -\rho\,\varepsilon & \eta_+ G_1^0 - \sqrt{1}\,\varepsilon & 0 & \eta_+^3 G_3^1 & 0 & \eta_+^5 G_5^2 & \ddots \\ \eta_- G_1^0 - \sqrt{1}\,\varepsilon & -\rho\,\varepsilon & \eta_+ G_2^0 - \sqrt{2}\,\varepsilon & 0 & \eta_+^3 G_4^1 & 0 & \ddots \\ 0 & \eta_- G_2^0 - \sqrt{2}\,\varepsilon & -\rho\,\varepsilon & \eta_+ G_3^0 - \sqrt{3}\,\varepsilon & 0 & \eta_+^3 G_5^1 & \ddots \\ \eta_-^3 G_3^1 & 0 & \eta_- G_3^0 - \sqrt{3}\,\varepsilon & -\rho\,\varepsilon & \eta_+ G_4^0 - \sqrt{4}\,\varepsilon & 0 & \ddots \\ 0 & \eta_-^3 G_4^1 & 0 & \eta_- G_4^0 - \sqrt{4}\,\varepsilon & -\rho\,\varepsilon & \eta_+ G_5^0 - \sqrt{5}\,\varepsilon & \ddots \\ \eta_-^5 G_5^2 & 0 & \eta_-^3 G_5^1 & 0 & \eta_- G_5^0 - \sqrt{5}\,\varepsilon & -\rho\,\varepsilon & \ddots \\ \ddots & \ddots & \ddots & \ddots & \ddots & \ddots & \ddots \end{pmatrix},$$

where G_n^s is evaluated at $z = -\sigma q^2 \lambda_{\mathrm{dB}}^2$, with $\sigma = \eta_-\eta_+$. These matrices enjoy properties opposite to those of $\mathbb{Q}_{\alpha\alpha}$. The substrate potential does appear (multiplying all elements in front of the matrices) while the force is absent. Besides, the matrices $\mathbb{Q}_{\alpha,\alpha\pm q}$ are independent of the index α, which permits to write them simply as $\mathbb{Q}^{\pm q}$. The only technical complication with respect to the common choice $\eta = 1/2$ is that we need to compute the Kummer functions ${}_1F_1(a, c; z)$ included in G_n^s, which in our case are simple polynomials (equation (C.12)). Note that to compute the observables we must eventually undo the momentum shift $p_\rho \to p = p_\rho + \rho$.

Appendix F. Semiclassical analytical results

In this appendix we derive some semiclassical formulae discussed in the main text.

F.1. Reflection and transmission for a saw-tooth barrier

In section 8.2, we invoked the current through a saw-tooth barrier deformed by $\pm Fx$ (figure F.1). We introduced the reflection coefficients $\mathcal{R}_+$ and $\mathcal{R}_-$ for $\pm F$. One has to analyse separately the cases of incident particles with energies above or below the barrier. In the first case, the reflection coefficient by a potential with a cusp (with slopes f_1 and f_2) is given by the first equation (45) ([62], section 52). Owing to the right slope in figure F.1 is infinity, we make it finite and finally take the vertical limit, getting

$$\frac{\mathcal{R}_+}{\mathcal{R}_-} = \frac{V_0 - FL}{V_0 + FL} < 1. \tag{F.1}$$

Next we consider the case of tunnelling through the barrier. The semiclassical transmission coefficient is also written in (45). Defining $A = |\int_a^b \mathrm{d}x\, p(x)|$, we calculate A_+ and A_- for positive and negative forces. After simple integrals, we find

$$\frac{A_+}{A_-} = \frac{V_0 + FL}{V_0 - FL}\left(\frac{V_0 - FL - E}{V_0 - E}\right)^{3/2} \tag{F.2}$$

with E the particle energy (cf [48]). For moderate forces, $F \leqslant 0.618 V_0/L$, we get for the transmission coefficients $\mathcal{T} = \exp[-(2/\hbar)A]$

$$A_+/A_- > 1 \qquad \rightsquigarrow \qquad \mathcal{T}_+/\mathcal{T}_- < 1. \tag{F.3}$$

Thus, for E below the barrier $\mathcal{R}_+/\mathcal{R}_- > 1$, while $\mathcal{R}_+/\mathcal{R}_- < 1$ for E above the barrier.

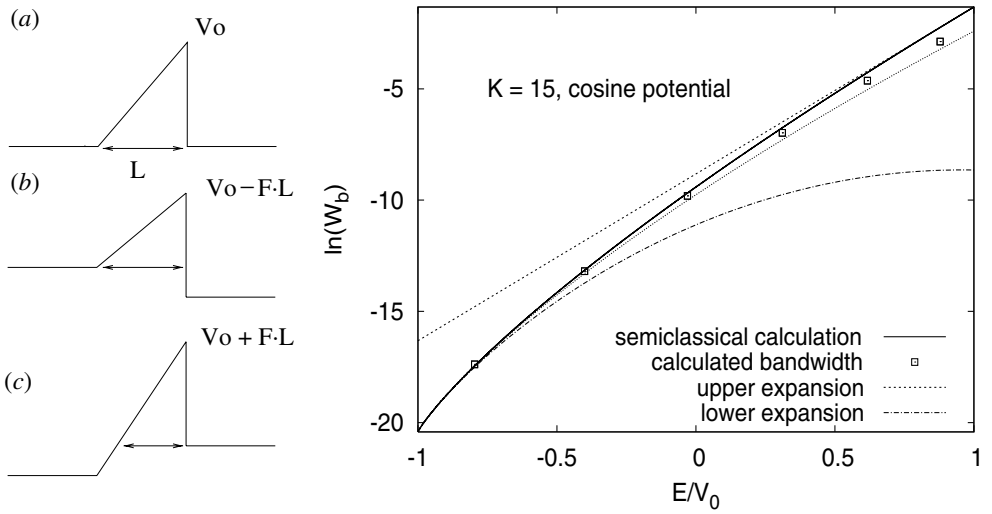

Figure F.1. Left panel: profile of the saw-tooth potential barrier for non-deformed (a) and deformed by $-Fx$ (b) and by $+Fx$ (c). Right panel: width of the energy bands W_b in a cosine potential (exact and various approximations).

F.2. Transmission coefficient and energy bands for a cosine potential

In order to get the semiclassical transmision coefficient through a potential $V(x) = -V_0 \cos(x/x_0)$, we need to integrate

$$A = \left| \int_a^b \mathrm{d}x \sqrt{2M[E + V_0 \cos(x/x_0)]} \right| \tag{F.4}$$

with turning points obeying $\cos(a/x_0) = \cos(b/x_0) = -E/V_0$. Due to $E + V_0 \cos(x/x_0) < 0$ below the barrier, we change the sign inside the square root extracting an i which is absorbed by the modulus. Simple transformations bring the integral into a tabulated form ([75], equation (2.576)), and we obtain

$$A = 4S_0[2\mathbf{E}(s) - (1+\varepsilon)\mathbf{K}(s)], \qquad \varepsilon = E/V_0, \qquad s = \sqrt{\tfrac{1}{2}(1-\varepsilon)}, \tag{F.5}$$

where $S_0 = \sqrt{MV_0x_0^2}$, and $\mathbf{K}(s)$ and $\mathbf{E}(s)$ are the first and second complete elliptic integrals ([37], chapter 5.8). Insertion in $\mathcal{T} = \exp[-(2/\hbar)A]$ gives the transmision coefficient through a cosine potential. This $\mathcal{T}$ also gives the *semiclassical energy bands* ([76], section 55)

$$E_q = E_0 \pm (\hbar\omega_0/\pi)\sqrt{\mathcal{T}}\cos(2\pi x_0 q), \tag{F.6}$$

with ω_0 the oscillation frequency in the wells. The width of the bands is therefore

$$W_\mathrm{b} = 2(\hbar\omega_0/\pi)\exp\{-4(S_0/\hbar)[2\mathbf{E}(s) - (1+\varepsilon)\mathbf{K}(s)]\}, \qquad \varepsilon = E/V_0. \tag{F.7}$$

The parameter s goes from 1 when $\varepsilon = -1$ (potential bottom) to 0 at the barrier top $\varepsilon = 1$. For $s \sim 1$ we can expand the elliptic integrals, obtaining

$$W_\mathrm{b} \simeq 2(\hbar\omega_0/\pi)\exp\Big[-(S_0/\hbar)\left(8 - (1+\varepsilon)\left\{1 + \ln\left[\tfrac{1}{32}(1+\varepsilon)\right]\right\}\right.$$
$$\left. +(1+\varepsilon)^2\left\{1 + \tfrac{1}{8}\ln\left[\tfrac{1}{32}(1+\varepsilon)\right]\right\}\right)\Big]. \tag{F.8}$$

At the potential bottom $\varepsilon = -1$ this gives $W_\mathrm{b} = \exp[-8(S_0/\hbar)]$. The bandwidth increases exponentially with the energy. Near the top, $\varepsilon \sim 1$, one has $s \sim 0$, and we can use the series expansion of the elliptic integrals, obtaining

$$W_\mathrm{b} \simeq 2(\hbar\omega_0/\pi)\exp[-\pi(S_0/\hbar)(1-\varepsilon)]. \tag{F.9}$$

Figure F.1 shows that equations (F.8) and (F.9) approximate well the exact results in their respective ranges (the later also serves as an upper bound). If we disregard the terms with $(1+\varepsilon)^2$ in (F.8), the result happens to fit remarkably W_b in all the range.

Appendix G. Perturbative solution for periodic forcing

Here we shall solve the following generic differential equation:

$$\tau\frac{\mathrm{d}\boldsymbol{c}}{\mathrm{d}t} + \mathcal{Q}\boldsymbol{c} = f(t)\mathcal{V}\boldsymbol{c}, \qquad f(t) = f_+\mathrm{e}^{+\mathrm{i}\omega t} + f_-\mathrm{e}^{-\mathrm{i}\omega t} \tag{G.1}$$

perturbatively in the forcing f. (For cosine forcing $f_+ = f_- = f/2$.) Comparing with section 9, we see that $\boldsymbol{c}$ corresponds to the vectors $\boldsymbol{c}_\alpha$, $\mathcal{Q}$ to the static part of the matrices $\mathbb{Q}_{\alpha\beta}$, and the perturbation $\mathcal{V}$ to $\Delta\mathbb{Q}_{\alpha\alpha}$, the part of $\mathbb{Q}_{\alpha\alpha}$ involving ΔF.

A periodic solution can be Fourier-expanded as

$$\boldsymbol{c} = C^{(0)} + \sum_{k=1}^{\infty}(f_+^k C^{(k)}\mathrm{e}^{+\mathrm{i}\omega_k t} + f_-^k\tilde{C}^{(k)}\mathrm{e}^{-\mathrm{i}\omega_k t}), \qquad \omega_k = k\omega \tag{G.2}$$

with $C^{(0)}$ the unperturbed response, while $\tilde{C}^{(k)} \neq C^{(k)*}$ for complex $\boldsymbol{c}$. Separating terms oscillating with $\mathrm{e}^{+\mathrm{i}\omega_k t}$ and $\mathrm{e}^{-\mathrm{i}\omega_k t}$, the left-hand side of (G.1) reads

$$\tau\frac{\mathrm{d}\boldsymbol{c}}{\mathrm{d}t} + \mathcal{Q}\boldsymbol{c} = \mathcal{Q}C^{(0)} + \sum_{k=1}^{\infty} f_+^k[\mathrm{i}(\omega_k\tau)C^{(k)} + \mathcal{Q}C^{(k)}]\mathrm{e}^{+\mathrm{i}\omega_k t} + \sum_{k=1}^{\infty} f_-^k[-\mathrm{i}(\omega_k\tau)\tilde{C}^{(k)} + \mathcal{Q}\tilde{C}^{(k)}]\mathrm{e}^{-\mathrm{i}\omega_k t}.$$

To obtain the right-hand side, we use $\omega_k \pm \omega = k\omega \pm \omega = \omega_{k\pm1}$, redefine the indices (keeping the same names) to get all the oscillating factors at $\pm\omega_k t$, and introduce the definition $\tilde{C}^{(0)} \equiv C^{(0)}$, arriving at

$$f(t)\mathcal{V}\boldsymbol{c} = f_+f_-(\mathcal{V}C^{(1)} + \mathcal{V}\tilde{C}^{(1)}) + \sum_{k=1}^{\infty} f_+^k[\mathcal{V}C^{(k-1)} + (f_+f_-)\mathcal{V}C^{(k+1)}]\mathrm{e}^{+\mathrm{i}\omega_k t} + \sum_{k=1}^{\infty} f_-^k[\mathcal{V}\tilde{C}^{(k-1)} + (f_+f_-)\mathcal{V}\tilde{C}^{(k+1)}]\mathrm{e}^{-\mathrm{i}\omega_k t}.$$

Equating terms with the same oscillating factors on both sides (*uniqueness* of the Fourier expansion), we obtain

$$\begin{aligned} &\mathcal{Q}C^{(0)} = \mathcal{V}[0 + (f_+f_-)(C^{(1)} + C^{(-1)})], \\ &\mathrm{i}(\omega_k\tau)C^{(k)} + \mathcal{Q}C^{(k)} = \mathcal{V}[C^{(k-1)} + (f_+f_-)C^{(k+1)}]. \end{aligned} \tag{G.3}$$

The $\tilde{C}^{(k)}$ are included as $C^{(-k)} \equiv \tilde{C}^{(k)}$ with $\omega_{-k} = -\omega_k$.

The contribution $\mathcal{V}C^{(k-1)}$ comes from products of 'rotating' terms $\mathrm{e}^{\pm\mathrm{i}\omega t} \times \mathrm{e}^{\pm\mathrm{i}\omega_k t}$. For instance, the oscillating factor $\mathrm{e}^{+\mathrm{i}\omega_{k-1}t}$ in $C^{(k-1)}$ when multiplied by the part $\mathrm{e}^{+\mathrm{i}\omega t}$ of the field raises the harmonic from $k-1$ to k. The term $\mathcal{V}C^{(k+1)}$ comes from products of 'counter-rotating' terms $\mathrm{e}^{\pm\mathrm{i}\omega t} \times \mathrm{e}^{\mp\mathrm{i}\omega_k t}$. For example, the product of the oscillating factor $\mathrm{e}^{+\mathrm{i}\omega_{k+1}t}$ and the

$e^{-i\omega t}$ part of the field lowers the order from $k+1$ to k. This contribution (the 'contamination' from higher harmonics) has an order higher in f than the contribution of $C^{(k-1)}$, which is therefore the leading one. Indeed, expanding the $C^{(k)}$ in powers of f we get the leading terms at each harmonic

$$\mathcal{Q}C^{(0)} = 0, \qquad i(\omega_k\tau)C^{(k)} + \mathcal{Q}C^{(k)} = \mathcal{V}C^{(k-1)}. \tag{G.4}$$

The $k = 0$ equation gives the static response (corresponding to equation (48)), $k = 1$ the linear dynamical response, etc (corresponding to equation (49)).

References

[1] Hillery M, O'Connell R F, Scully M O and Wigner E P 1984 *Phys. Rep.* **106** 121
[2] Lee H-W 1995 *Phys. Rep.* **259** 147
[3] Schleich W P 2001 *Quantum Optics in Phase Space* (Berlin: Wiley–VCH)
[4] Balescu R 1991 *Equilibrium and Nonequilibrium Statistical Mechanics* reprinted edn (Malabar, FL: Krieger)
[5] Zurek W H 1991 *Phys. Today* **44** 36
[6] Grabert H, Schramm P and Ingold G-L 1988 *Phys. Rep.* **168** 115
[7] Weiss U 1993 *Quantum Dissipative Systems* (Singapore: World Scientific)
[8] Breuer H-P and Petruccione F 2002 *The Theory of Open Quantum Systems* (Oxford: Oxford University Press)
[9] Guinea F, Bascones E and Calderón M J 1998 *Lectures on the Physics of Highly Correlated Electrons* ed F Mancini (New York: AIP)
[10] Wallraff A, Lukashenko A, Lisenfeld J, Kemp A, Fistul M V, Koval Y and Ustinov A V 2003 *Nature (London)* **425** 155
[11] Kohen D, Marston C C and Tannor D J 1997 *J. Chem. Phys.* **107** 5236
[12] Klein O 1921 *Arkiv för Matematik, Astronomi och Fysik* **16** 1
[13] Kramers H A 1940 *Physica* **7** 284
[14] Risken H 1989 *The Fokker–Planck Equation* 2nd edn (Berlin: Springer)
[15] Balescu R 1997 *Statistical Dynamics* reprinted 2000 edn (London: Imperial College Press)
[16] Brinkman H C 1956 *Physica* **22** 29
[17] Kalmykov Y P and Coffey W T 1997 *Phys. Rev.* B **56** 3325
[18] Stockburger J T 2003 *Phys. Status Solidi* b **237** 146
[19] Ford G W, Lewis J T and O'Connell R F 1988 *Phys. Rev.* A **37** 4419
[20] Shibata F 1980 *J. Phys. Soc. Japan* **49** 15
[21] Shibata F and Uchiyama C 1993 *J. Phys. Soc. Japan* **62** 381
[22] Vogel K and Risken H 1988 *Phys. Rev.* A **38** 2409
Vogel K and Risken H 1989 *Phys. Rev.* A **39** 4675
[23] Tan S M 1999 *A Quantum Optics Toolbox for Matlab 5* http://www.qo.phy.auckland.ac.nz/html/qotoolbox.html
Tan S M 1999 *J. Opt. B: Quantum Semiclass. Opt.* **1** 424
[24] García-Palacios J L 2004 *Europhys. Lett.* **65** 735 (*Preprint* cond-mat/0406047)
[25] Caldeira A O and Leggett A J 1983 *Physica* A **121** 587
[26] Tanimura Y and Wolynes P G 1991 *Phys. Rev.* A **43** 4131
[27] Hu B L, Paz J P and Zhang Y 1992 *Phys. Rev.* D **45** 2843
[28] Anastopoulos C and Halliwell J J 1995 *Phys. Rev.* D **51** 6870
[29] Cohen D 1997 *Phys. Rev. Lett.* **78** 2878
[30] Zurek W H and Paz J P 1994 *Phys. Rev. Lett.* **72** 2508
[31] Karrlein R and Grabert H 1997 *Phys. Rev.* E **55** 153
[32] Kohler S, Dittrich T and Hänggi P 1997 *Phys. Rev.* E **55** 300
[33] Ankerhold J 2003 *Irreversible Quantum Dynamics* (*Lectures Notes in Physics* vol 622) ed F Benatti and R Floreanini (New York: Springer) p 165
[34] Ankerhold J 2003 *Europhys. Lett.* **61** 301
Machura L *et al* 2004 *Phys. Rev.* E **70** 031107 (*Preprint* cond-mat/0402116)
[35] Isar A, Sandulescu A and Scheid W 1996 *Int. J. Mod. Phys.* B **10** 2767
[36] Galindo A and Pascual P 1990 *Quantum Mechanics* vol I (Berlin: Springer)
[37] Arfken G 1985 *Mathematical Methods for Physicists* 3rd edn (Boston, MA: Academic)
[38] Ploszajczak M and Rhoades-Brown M J 1985 *Phys. Rev. Lett.* **55** 147
[39] Lill J V, Haftel M I and Herling G H 1989 *J. Chem. Phys.* **90** 4940
[40] Johansen L M 1998 *Phys. Rev. Lett.* **80** 5461

[41] Burghardt I and Møller K B 2002 *J. Chem. Phys.* **117** 7409
[42] Hug M, Menke C and Schleich W P 1998 *J. Phys. A: Math. Gen.* **31** L217
[43] Monteoliva D and Paz J P 2001 *Phys. Rev.* E **64** 056238
[44] Tanimura Y and Wolynes P G 1992 *J. Chem. Phys.* **96** 8485
[45] Schmid A 1983 *Phys. Rev. Lett.* **51** 1506
[46] Guinea F, Hakim V and Muramatsu A 1985 *Phys. Rev. Lett.* **54** 263
[47] Fisher M P A and Zwerger W 1985 *Phys. Rev.* B **32** 6190
[48] Reimann P 2002 *Phys. Rep.* **361** 57
[49] Glück M, Kolovsky A R and Korsch H J 2002 *Phys. Rep.* **366** 103
[50] Jung P 1993 *Phys. Rep.* **234** 175
[51] Ferrando R, Spadacini R, Tommei G E and Caratti G 1993 *Physica* A **195** 506
[52] Asaklil A, Mazroui M and Boughaleb Y 1999 *Eur. Phys. J.* B **10** 91
[53] Kandemir B S 1998 *Phys. Lett.* A **245** 209
[54] Chen Y-C and Lebowitz J L 1992 *Phys. Rev.* B **46** 10751
[55] Chen Y-C and Lebowitz J L 1992 *Phys. Rev. Lett.* **69** 3559
[56] Ozorio de Almeida A M 1998 *Phys. Rep.* **295** 265
[57] Reimann P, Grifoni M and Hänggi P 1997 *Phys. Rev. Lett.* **79** 10
[58] Grifoni M, Ferreira M S, Peguiron J and Majer J B 2002 *Phys. Rev. Lett.* **89** 146801
[59] Scheidl S and Vinokur V M 2002 *Phys. Rev.* B **65** 195305
[60] Bartussek R, Hänggi P and Kissner J G 1994 *Europhys. Lett.* **28** 459
[61] Mel'nikov V I 1991 *Phys. Rep.* **209** 1
[62] Landau L D and Lifshitz E M 1965 *Quantum Mechanics* 2nd edn (Oxford: Pergamon)
[63] Linke H, Humphrey T E, Lindelof P E, Löfgren A, Newbury R, Omling P, Sushkov A O, Taylor R P and Xu H 2002 *Appl. Phys.* A **75** 237
[64] Titantah J T and Hounkonnou M N 1999 *J. Phys. A: Math. Gen.* **32** 897
[65] Gekht R S 1983 *Fiz. Met. Metalloved.* **55** 225
Gekht R S 1983 *Phys. Met. Metallogr. (USSR)* **55** 12 (Engl. Transl.)
[66] Garanin D A, Ishchenko V V and Panina L V 1990 *Teor. Mat. Fiz.* **82** 242
Garanin D A, Ishchenko V V and Panina L V 1990 *Theor. Math. Phys.* (*USSR*) **82** 169 (Engl. Transl.)
[67] Feynman R P 1972 *Statistical Mechanics: A Set of Lectures* (*Frontiers in Physics* vol 10) (Reading, MA: Benjamin)
[68] Balucani U, Lee M H and Tognetti V 2003 *Phys. Rep.* **373** 409
[69] Bender C M and Milton K A 1994 *J. Math. Phys.* **35** 364
[70] Jung P and Risken H 1985 *Z. Phys.* B **59** 469
[71] Coffey W T, Kalmykov Y P and Waldron J T 1994 *Physica* A **208** 462
[72] Huang Y and McColl W F 1997 *J. Phys. A: Math. Gen.* **30** 7919
[73] Press W H, Teukolsky S A, Vetterling W T and Flannery B P 1992 *Numerical Recipes* 2nd edn (New York: Cambridge University Press)
[74] Pathak A 2000 *J. Phys. A: Math. Gen.* **33** 5607
[75] Gradshteyn I S and Ryzhik I M 1994 *Table of Integrals, Series, and Products* 5th edn (San Diego, CA: Academic)
[76] Lifshitz E M and Pitaevskiĭ L P 1980 *Statistical Physics* (Part 2) (Oxford: Pergamon)